PRODUCTION OF POLYMERIC MIXED MATRIX MEMBRANES WITH INCORPORATION OF ACTIVATED CARBON DERIVED FROM EXTRACTED OLIVE POMACE FOR WASTEWATER TREATMENT

Evelyn Fernanda Latarulo de Moraes

Dissertation submited to Escola Superior Agrária de Bragança to obtain the Degree of Master in Environmental Technology in the context of the double degree program with the Federal Technological University of Paraná.

Supervised by

Prof. Dr. Helder Teixeira Gomes
Prof. Fabio Orssatto

Bragança
2024

Funding: The authors would like to thank the Foundation for Science and Technology (FCT, Portugal) for financial support through national funds FCT/MCTES (PIDDAC) to CIMO (UIDB/00690/2020 and UIDP/00690/2020), SusTEC (LA/P/0007/2020), and to project "BagaÇo+Valor – Clean technology for recovering olive pomace by-product in the olive oil extraction industry – (NORTE-01-0247-FEDER-072124).

ACKNOWLEDGMENTS

I express my profound gratitude to God for His infinite wisdom and kindness, which have guided my steps and provided countless learning opportunities throughout this academic journey.

I am deeply thankful to Prof. Helder Teixeira Gomes and Prof. Fábio Orssatto for their wisdom, guidance, and fundamental contributions to the development of this work.

To my father, mother, and sister, I dedicate my eternal gratitude for their unconditional support in every moment of my life, always being my pillar of strength.

I would like to extend my gratitude to my dear friends from UTFPR-MD, especially Alexandre, Heitor, Luis Felipe, Matheus, Renata, Helen, Jonathan, and Thiago, whose presence and support were essential at every stage of this journey.

I would also like to thank the friends from Portugal who always provided the best everyday experiences, sharing life experiences. In particular, I would like to acknowledge Nayara, Lorena, and Caroline, who have always been present and supportive in the most complex moments.

I would like to express my profound gratitude to Ana, who played a pivotal role in the development of this dissertation. Her invaluable guidance and companionship were instrumental in enabling me to complete this work.

I would like to express my gratitude to Adriano, Fernanda, and Maria João for the invaluable experience and insights gained from sharing experiences in the workplace and beyond.

I would like to express my sincerest gratitude to Professor José Luis Díaz de Tuesta and the Chemical and Environmental Engineering Group (ESCET) at the Universidad Rey Juan Carlos for their invaluable support and assistance during the preparation of this dissertation. Their guidance and support were of the utmost importance in enabling me to complete this work.

I would also like to extend my profound acknowledgment to all my family, friends, and teachers who have played a role in my personal and professional growth.

In memory of Professor Dalesio, who was an inspiration and encouraged me to pursue the path of research.

I would like to express my gratitude to the Federal Technological University of Paraná and the Polytechnic Institute of Bragança for providing me with the opportunity to expand my knowledge alongside dedicated professors and collaborators.

I would also like to thank all those mentioned and many others who contributed to this work in some way.

"Great achievements are possible
when attention is paid
to small beginnings."
– Lao Tzu

ABSTRACT

The European Union is the world's largest producer, consumer and exporter of olive oil. Consequently, olive pomace, a by-product of olive oil production, is generated in abundance and, when disposed incorrectly, can cause negative impacts to the environment. Despite being a severe environmental problem, olive pomace is a precious resource of valuable compounds for recovery and valorization. One alternative for valorization is the production of activated carbon materials produced via pyrolysis of biomass, followed with activation by physical, chemical or physicochemical methods, developing high porosity, which improves adsorption capacity for wastewater treatment. In this study, activated carbons are developed from olive pomace by pyrolysis and activation with CO_2 injection (AC_CO_2), resulting in a material with a high surface area and adsorptive capacity. To make these materials more attractive, they can be incorporated into polymeric membranes, which can be used in filtration systems for wastewater treatment. Thus, this study focuses on incorporating activated carbons in polymeric membranes to be used in the recovery of phenolic compounds such as phenol.

Keywords: Olive pomace; activated carbons; polymeric membranes; wastewater treatment

RESUMO

A União Europeia é o maior produtor, consumidor e exportador de azeite do mundo. Consequentemente, o bagaço de azeitona, um subproduto da produção de azeite, é gerado em abundância e, quando eliminado incorretamente, pode causar impactos negativos para o ambiente. Apesar de ser um grave problema ambiental, o bagaço de azeitona é um recurso precioso de compostos valiosos para recuperação e valorização. Uma alternativa de valorização é a produção de materiais de carbono ativado produzidos através da pirólise da biomassa, seguida de ativação por métodos físicos, químicos ou físico-químicos, desenvolvendo uma elevada porosidade, o que melhora a capacidade de adsorção para o tratamento de águas residuais. Neste estudo, os carvões ativados são desenvolvidos a partir de bagaço de azeitona por pirólise e ativação com injeção de CO_2 (AC_CO_2), resultando num material com elevada área de superfície e capacidade adsorvente. Para tornar estes materiais mais atrativos, podem ser incorporados em membranas poliméricas, que podem ser utilizadas em sistemas de filtração para tratamento de águas residuais. Por conseguinte, o presente estudo visa incorporar carvões ativados em membranas poliméricas para serem utilizados na recuperação de compostos fenólicos como o fenol.

Palavras chave: bagaço de azeitona; carvões ativados; membranas poliméricas; tratamento de águas residuais

SUMMARY

1. Introduction **1**

2. State of the art **2**

2.1 Olive Oil Production 2

2.2. Olive Oil Extraction Industry 2

2.2.1. Dried Extracted Olive Pomace 4

2.2.2. Wastewater from Olive Pomace Oil Extraction Industries 5

2.3. Olive Mill WasteWater Processes of Olive Pomace Oil Extraction Industries 7

2.3.1. Valorization of Extracted Olive Pomace 7

2.3.1.1. Valorization of Olive Pomace in the Pyrolysis Process 8

2.3.1.1.1. Activated carbon 9

2.3.1.2. Wastewater Treatment Systems of the Olive Pomace Oil Extraction Industry 10

2.3.1.2.1. Membrane Utilization in Wastewater Treatment 11

2.4 Types of polymeric membranes 13

3. Objectives **16**

3.1 Specific Objectives 16

4. Materials and Methods **17**

4.1 Reactants and equipaments 17

4.1.1 Reactants 17

4.1.2 Equipaments 17

4.2 Methods 17

4.2.1 Production of Activated Carbon and Polymeric Membrane 17

4.2.1.1 Synthesis of Activated Carbon (AC_CO_2) 17

4.2.1.2 Preparation of Polymeric Membranes 18

4.2.1.2.1 Experimental Design 18

4.2.1.2.2 Production of Polymeric Membranes 20

4.2.2 Characterization of Materials 22
4.2.2.1 Elemental analysis (CHNS) 22
4.2.2.2 Ash Content 22
4.2.2.3 pH Point of Zero Charge Determination 23
4.2.2.4 Acid-Base Characterization 23
4.2.2.5 Porosimetry and surface area 24
The surface area is a critical information in 24
4.2.2.6 Determination of Surface Chemistry 24
4.2.2.7 Thermogravimetric Analysis 24
4.2.2.8 Morphological Analysis 24
4.2.3 Analysis and Application Methods 25
4.2.3.1 Kinetics and adsorption isotherms with AC_CO_2 25
4.2.3.1.1 Kinetic models 26
4.2.3.1.2 Equilibrium isotherms 26
4.2.3.1.2.1 Equilibrium isotherms models 26
4.2.3.2 Filtration with Polymeric Membranes 27
4.2.3.2.1 High Performance Liquid Chromatography (HPLC) 28
5. Results and discussion 30
5.1 Characterization of AC_CO_2 30
5.1.1 Elemental Analysis 30
5.1.2 Adsorption Experiments 30
5.1.2.1 Kinetic models 30
5.1.2.2 Equilibrium isotherms 32
5.2 Preparation and incorporation of polymeric membranes 33
5.2.1 Response surface analysis 33
5.3 Characterization of materials 36

5.3.1 Porosity Characterization 36

5.3.2 Thermogravimetric Analysis 38

5.3.3 Fourier-transform infrared spectroscopy 40

5.3.4 Contact angle and pHpzc 42

5.3.5 The surface morphology 43

5.3.6 Analysis of Polymeric Membranes in a Continuous System 46

6. Conclusions 48

7. Future works suggestions 50

8. References 51

FIGURE LIST

Figure 1 - Olive oil extraction process using the three-phase method and pressing. 3
Figure 2 - The olive oil extraction process using the two-phase method. 3
Figure 3 - Flowchart of the conventional effluent treatment process. 11
Figure 4 - Flowchart of the wastewater treatment process with membrane filtration. 12
Figure 5 - Scheme of the slow pyrolysis process for the production and activation of carbon 18
Figure 6 - BBD for 3 independent variables 19
Figure 7 - Schematic diagram for membrane preparation 22
Figure 8 - Adsorption isotherms[123] 25
Figure 9 - Structural diagram for the membrane filtration system. 28
Figure 10 - Calibration curve for phenol measurements 29
Figure 11 - Fitting the kinetic models to the experimental data for AC-CO_2. 31
Figure 12 - Experimental results for phenol adsorption using the Langmuir and Freundlich isotherm models 32
Figure 13 – Polymeric membrane of: a) formulation 8 with activated carbon; b) formulation 14 with activated carbon 34
Figure 14 - Polymeric membrane of: a) formulation 4 with activated carbon; b) formulation 5 with activated carbon 35
Figure 15 - Polymeric membrane of: a) formulation 2 with activated carbon; b) formulation 6 with activated carbon 35
Figure 16 - Polymeric membrane of: a) formulation 8; b) formulation 14 36
Figure 17 - N_2 adsorpition-desorption isotherms at 77 K from AC_CO_2 37
Figure 18 - a) N_2 adsorption-desorpition at 77 K from AC_CO_2 M8; b) from M8 37
Figure 19 - a) N_2 adsorption-desorpition at 77 K from AC_CO_2 M14; b) from M14 38
Figure 20 - a) Thermogravimetric analysis of olive pomace; b) Thermogravimetric analysis of activated carbon 39
Figure 21 - Thermogravimetric Analysis membranes 40
Figure 22 - FTIR Characterization for Polymeric Membrane with Activated Carbon 41
Figure 23 - pH point of zero charge: AC_CO_2, AC_CO_2 M8 and M8. 43
Figure 24 - Scanning Electron Microscopy of Polymeric Membrane 8. 44
Figure 25 - Scanning Electron Microscopy of Polymeric Membrane 14. 44
Figure 26 - Scanning electron microscopy was used to examine the polymeric membrane 8 with activated carbon. 45

Figure 27 - Scanning Electron Microscopy of Polymeric Membrane 14 with Activated Carbon Incorporation 46
Figure 28 - Removal of phenol by polymeric membrane with AC-CO_2 47

TABLE LIST

Table 1 - Physical-chemical characteristics of the extracted pomace. 5
Table 2 - Characterization of OMWW. 6
Table 3 - Industrial Wastewater Discharge Parameters. 7
Table 4 - Pore Classification According to IUPAC[78] 10
Table 5 - Experimental variables and their levels used in the BBD. 19
Table 6 - Box–Behnken design layout 20
Table 7 - The quantity of reagents for the formulation of polymeric membranes incorporating activated carbon. 21
Table 8 - Elemental analysis of CNHS for EOP and AC-CO_2 30
Table 9 - Parameters of the kinetic models for the activated carbon. 31
Table 10 - Parameters of equilibrium models: Langmuir and Freundlich 32
Table 11 - Response surface analysis 33
Table 12 - Textural properties of EOP, AC-CO_2 and Polymeric Membranes. 36
Table 13 - Contact angle and pHpzc 42

LIST OF ACRONYMS

EOP	Extracted Olive Pomace
BET	Brunauer, Emmett and Teller
AC_CO_2	Activated Carbon with carbon dioxide
PCs	Phenolic Compounds
CQD	Chemical Oxygen Demand
GG	Greenhouse Gases
OPOEI	Olive Pomace Oil Extraction Industry
IUPAC	International Union of Pure and Applied Chemistry
MF	Microfiltration
NF	Nanofiltration
RO	Reverse Osmosis
pH_{PZC}	pH at the Point of Zero Charge
PVP	Polyvinylpyrrolidone
RGCA	Gravimetric Yield of Carbonization
TGA	Thermogravimetric Analysis
UE	European Union

UF	Ultrafiltration
MAV	Maximum Allowable Value
RMV	Recommended Maximum Value
ELV	Emission Limit Value
μm	Micrometer
OMWW	Olive Mill WasteWater
PVDF	Polyvinylidene fluoride
NMP	1-Methyl-2-pyrrolidone

1. INTRODUCTION

The environmental challenges of the 21st century are central topics in global political agendas, focusing on energy reuse, waste valorization, greenhouse gas reduction, and the utilization of clean energies[1]. The objective is to control climate change and resource depletion. This control aims to promote a healthy quality of human life, ensuring access to environmental resources for future generations and enabling sustainable development.

Olive oil production worldwide is continuously expanding due to consistent consumption in recent years, driven by the popularity of "Mediterranean diets," which promote a healthy lifestyle due to the associated benefits[2]. As a result, the European Union produces approximately 2 million tons annually, with Spain, Italy, Greece, and Portugal being the major olive oil producers in the region.

The olive oil extraction process can be done using three different methodologies: mechanical pressing, two-phase centrifugation, and three-phase centrifugation[3,4]. Each extraction method generates by-products, such as olive pomace (OP) and olive mill wastewater (OMWW)[5,6]. The liquid waste generated has significant pollutant potential, leading to various environmental burdens, including soil contamination, hindrance of plant development, water body pollution, leaching of pollutants like phenolic compounds into groundwater, and disruption of aquatic ecosystems[7]. The OP has about 55 to 70% moisture content and approximately 2 to 3% oil content. It can be sent to Olive Pomace Oil Extraction Industriy (OPOEI), where, through the use of a solvent (n-hexane), the remaining oil is removed, leaving behind only dried and extracted OP, which can be directed for valorization or energy recovery[8].

This study aims to valorize the extracted olive pomace (EOP) residue generated by OPOEI through recovery via the slow pyrolysis process with CO_2 injection to develop activated carbon porosity. This activated carbon will be incorporated into the manufacturing process of polymeric membranes due to its affinity for phenolic compounds, especially phenol. This incorporation aids in the adsorption and filtration of model wastewater. The phenol can be recovered and used in the pharmaceutical and cosmetic industries, reducing the need for new natural resources.

2. STATE OF THE ART

2.1 Olive Oil Production

The olive tree (*Olea Europaea* L.) is cultivated for olive oil production. It constitutes one of the leading agricultural activities in Mediterranean countries (Spain, Italy, Greece, and Portugal) due to the favorable edaphoclimatic conditions in the region, making it the world's largest producer[9]. Olive oil is considered a healthy fat and has experienced consistent consumption in recent years due to the popularity of "Mediterranean diets", promoting a healthy lifestyle[2]. Various studies have reported beneficial effects of olive oil from different cultivars on human health[10], such as anti-inflammatory properties, prevention of cardiovascular diseases, cholesterol reduction, and decreased risk of diabetes[11–13].

Cultivating olive trees provides several societal benefits beyond their economic importance, including improved quality of life from olive oil consumption, landscape maintenance and enhancement, and ecological and environmental services[14,15]. Global olive oil production has been steadily increasing, rising from 2.83 million tons in 2008-2009 to 3.23 million tons in 2019-2020, representing a growth of approximately 14%[16,17]. The European Union (EU) produces around 2 million tons annually, with Spain (66%), Italy (15%), Greece (13%), and Portugal (5%) being its major producers[18].

Portugal has the potential to become the world's third-largest olive oil producer due to modernization in olive grove cultivation, improved production practices through intensive and mechanized methods, increased harvest yield, and reduced operational costs[3]. The northern region of Portugal accounts for approximately 15% of the country's olive production, yielding about 650 thousand tons of OP, a pasty residue with high moisture content. However, its composition can be influenced by the extraction method used[19]. Typically, the produced OP has limited economic value; nevertheless, reuse practices are increasingly adopted, such as extracting the remaining 2 to 3% of oil, a common practice in olive pomace oil extraction industries[20].

2.2. Olive Oil Extraction Industry

Olive oil extraction can occur through three distinct methodologies: mechanical pressing, two-phase centrifugation, and three-phase centrifugation[3,4]. The pressing method, the oldest of the three, is based on extracting olive juice through mechanical or hydraulic pressure, generating the oily must that is then directed for spontaneous decantation or centrifugation, resulting in the separation of oil and moist pomace. However, this method

has low production efficiency and high labor costs[21]. The three-phase centrifugation method involves oil separation and includes basic steps such as debris removal, washing, crushing, beating, and vertical centrifugation. This system heavily relies on the moisture content in olives, as if necessary, a portion of water is added to facilitate extraction, leading to a significant volume of wastewater (Figure 1) [22,23] .

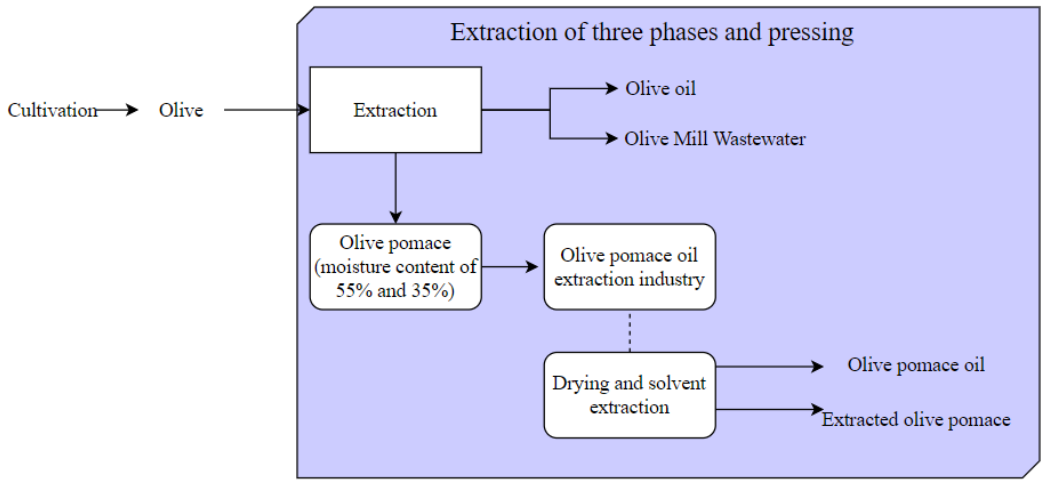

Figure 1 - Olive oil extraction process using the three-phase method and pressing.

The two-phase centrifugation method does not involve adding water, thereby reducing wastewater generation at the end of the process. In this procedure, olives are crushed and separated into oil and a mixture of water and pulp. Two by-products are obtained from this process: olive oil and EOP (Figure 2). Due to its water-free extraction process, this method is more appealing due to its energy efficiency, cost-effectiveness, and reduced water consumption.

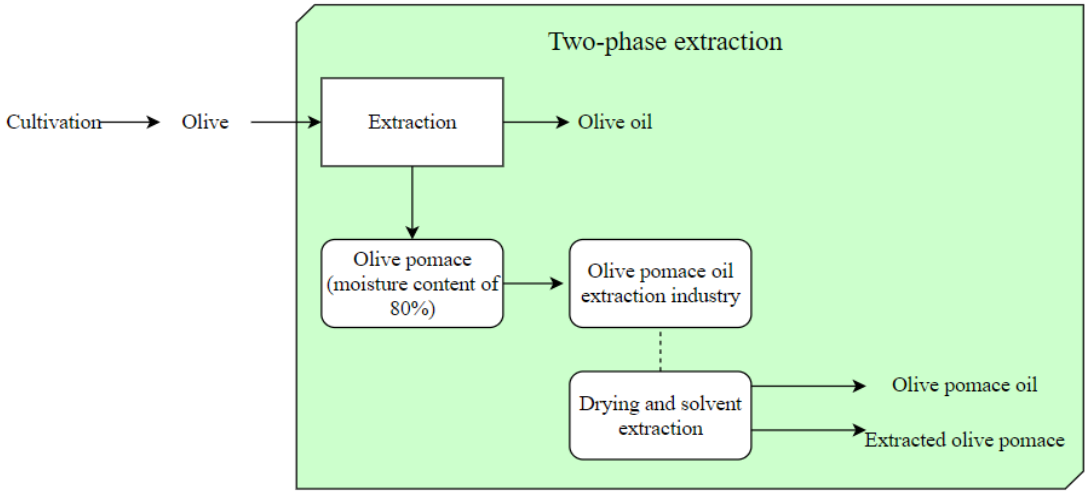

Figure 2 - The olive oil extraction process using the two-phase method.

Both methodologies generate by-products such as EOP and OMWW[5,24]. However, what sets the methods apart is the volume produced at the end of the extraction process. When these liquid or solid residues are not properly treated or reused, they can lead to a series of environmental problems, such as soil contamination, hindering plant development, or water body pollution, leaching pollutants like phenolic compounds into groundwater and other water bodies, hampering the self-purification process, ecological balance, and imparting color and odor[7].

The wet pomace resulting from the two-phase olive oil extraction process is characterized as a thick residue containing small amounts of pits and pulp, with a moisture content ranging from 55% to 70% and about 3% to 4% fat content[25]. To valorize this residue, it is sent to the OPOEI, where, using the solvent n-hexane, it can achieve a yield of 21.7% of residual oil, which is subsequently refined for human consumption[26,27]. After the extraction process, the EOP is directed for drying. In Portugal, approximately 129,000 tons of dry pomace are generated annually. This residue can undergo various forms of valorization or be used as biomass for burning, serving as a source of heat in drying processes, or being commercialized for combustion in other industries[23,28].

2.2.1. Dried Extracted Olive Pomace

Virgin pomace is a by-product generated during the initial olive oil extraction, containing notable levels of water (24%) and oil (9%)[29,30]. Wet pomace is produced in a two-phase and three-phase hydraulic press and centrifugation systems[31], while extracted pomace is a residue obtained after extracting oil from OP using n-hexane[29]. Lastly, dried extracted pomace is a residue obtained in extraction units after removing the residual oil from dry pomace. The physicochemical characterization of the extracted EOP found in the literature is presented in Table 1.

Table 1 - Physical-chemical characteristics of the extracted pomace.

Characterization	Extracted Olive Pomace
Direct Analysis (% Weight)	
Carbon	22.13
Volatile Matter	72.29
Ash	4.58
Moisture	12.69
Elemental Analysis (% Weight)	
Carbon	50.54
Hydrogen	5.86
Nitrogen	0.97
Sulfur	0.07
Oxygen	42.56
Calorific Value (kcal/kg Dry)	
Higher	4500
Lower	4300

EOP is a residue composed of the pulp and epicarp of the fruits produced in olive oil extraction units. Chemically, it consists of two types of components: structural and non-structural[29]. Structural elements include polysaccharides like cellulose, hemicellulose, and lignin, which comprise insoluble polymeric macromolecules responsible for forming cell walls and imparting shape and chemical and physical properties to the material. Lignin represents approximately 40% of the pomace's mass[32]. On the other hand, non-structural components are compounds with low degrees of polymerization, or even non-polymerized, characterized by low molecular weight and can be removed through solvent solubilization processes. These components encompass a variety of organic chemical families and compounds such as n-alcohols, waxes, fatty acids, sterols, phenols, and polyphenols[5,32].

2.2.2. Wastewater from Olive Pomace Oil Extraction Industries

Industrial wastewater originates from various activities and does not fall under domestic or rainwater wastewater. These wastewaters contain a variety of organic, inorganic, biological, and toxic pollutants[33]. Discharging these untreated wastewaters into the natural environment can lead to severe imbalances in the aquatic ecosystem, as they consume oxygen during decomposition, potentially causing the death of microorganisms and fish. Additionally,

nutrients such as phosphorus and nitrogen can trigger the eutrophication process[7,34]. The characterization of OMWW can be found in Table 2.

Table 2 - Characterization of OMWW.

Parameter		**Concentration**
pH	4.8	Sorensen Scale
COD	50.4	g de O_2 L^{-1}
BOD_5	8	g de O_2 L^{-1}
Total Suspended Solids	0.6	g L^{-1}
Total Volatile Solids	15.3	g L^{-1}
Total Solids	27.4	g L^{-1}
Total Polyphenols	4.3	g L^{-1}

The chemical composition of OMWW is influenced by various parameters, including maturation time, olive tree type, region, and variety, as well as the extraction method employed. Each method plays a significant role in the wastewater's composition, leading to variations in the chemical characteristics of OMWW[35].

According to Davies[36], the wastewater from olive pomace oil extraction units can contain 83-94% water, an inorganic or mineral fraction (metal ions) of 4-16%, and an organic fraction of 0.4-2.5%. The organic fraction comprises a significant composition of phenolic compounds. This industrial wastewater has high levels of suspended solids, odor, turbidity, low biodegradability, and high organic content, mainly concerning COD (Chemical Oxygen Demand). It also contains a high concentration of phenolic compounds (PCs), with over 50 types identifiable, imparting a dark color and bactericidal character to the wastewater, complicating biological treatment. Due to their challenging degradability (toxic to most microorganisms), acidic pH (3-6), and high organic load, discharging them into the environment can lead to severe impacts, such as altering the color of natural waters, modifying soil quality, changing microbial characteristics, and inducing phytotoxicity[2,37,38].

The olive contains a significant amount of PCs in its composition, of which about 2% remain in the olive oil after the extraction process, resulting in an wastewater with 98% PCs[39]. Consequently, the generated OMWW exhibits high concentrations of these compounds,

reducing the effectiveness of possible biological treatments. The permitted concentrations for the discharge of industrial wastewater into the sewer system are regulated by Decree-Law No. 236/98[40] and the General Regulation for Collection, Treatment, and Discharge of Wastewaters[41], as presented in Annex II, for parameters such as pH, COD, TSS, oils and fats, sulfides, and phenolic compounds. These values must not exceed the Maximum Allowable Limits (MAL), Recommended Maximum Values (RMV), and Emission Limits (EL), as indicated in Table 3.

Table 3 - Industrial Wastewater Discharge Parameters.

Parameter	**Unit**	**ELV**	**RMV**	**MAV**
Temperature	ºC	40	-	-
pH	Sorensen Scale	-	$6 \leq pH \leq 9$	$4.5 \leq pH \leq 10$
BOD_5 at 20ºC	mg O_2 L^{-1}	500	-	-
COD	mg O_2 L^{-1}	-	1000	2000
Total Suspended Solids (TSS)	mg L^{-1}	-	500	1000
Oils and Fats	mg L^{-1}	-	50	100
Phenolic Compounds	mg (C_6H_5OH) L^{-1}	-	20	40
Sulfides	mg L^{-1}	-	10	20

However, PCs offer advantages due to their low molecular weight. These compounds can be recovered and utilized at appropriate concentrations in various industrial sectors, including food, cosmetics, and pharmaceuticals, owning to their health benefits such as cardio protective, anti-inflammatory, and antioxidant properties, among others[42]. This makes them valuable raw materials for recovery, with zero cost and environmental benefits, especially in recycling processes. Therefore, utilizing by-products from the olive oil extraction industry is highly advisable[8].

2.3. Olive Mill WasteWater Processes of Olive Pomace Oil Extraction Industries

2.3.1. Valorization of Extracted Olive Pomace

In the literature, the most common methods for valorizing residual biomass from OPOEI include recovering bioactive compounds, which are biomolecules naturally present in olives

and lost during oil extraction. These bioactive compounds have health benefits and can be incorporated into bioeconomic, pharmaceutical, or cosmetic sectors[43]. Composting emerges as an alternative for waste valorization, offering sustainable management and the production of high-quality compost that aids in plant development. However, careful attention is crucial during the composting process; if quality is not maintained, toxins may be released into the soil, leading to nitrogen immobilization and inhibiting plant growth[44]. Composting is a biological aerobic process in which microorganisms convert biodegradable organic matter into humidified material[39].

Furthermore, EOP is being studied for its application in manufacturing materials for the construction industry, such as incorporation into clay bricks for developing eco-friendly ceramic materials[45]. Another application in the construction sector involves using EOP as a sustainable antioxidant, serving as a material recycling agent for asphalt pavement, where EOP has been processed to modify asphalt binder, enhancing crack resistance[46].

The production of biofuels using the waste from OPOEI is currently a highly sought-after alternative, with several technologies available to valorize this waste. Scientific studies explore opportunities to utilize these residues in producing electrical and thermal energy through synthesis gas, even fueling biomass thermal power plants[47]. Additionally, research is being conducted on biogas production[44] and biomass pyrolysis[48,49].

Biomass in energy recovery is of great interest to national and international energy markets[6]. The high calorific value of biomass makes it an ideal solid fuel for electricity generation. It is employed to fuel boilers that produce steam, utilized in composting processes, and biomass valorization through pyrolysis, thus promoting the adoption of Waste-to-Energy technologies. This concept encompasses waste incineration and various treatment processes aimed at generating energy, either in the form of electricity or heat[50,51].

The circular economy is a fundamental strategic concept aimed at reducing, reusing, recovering, and recycling materials and energy, fostering sustainable economic development, and the more efficient use of natural resources[52]. Therefore, adopting an appropriate model for managing olive oil waste is crucial, encouraging its valorization and contributing to the circular economy[53].

2.3.1.1. Valorization of Olive Pomace in the Pyrolysis Process

The pyrolysis process typically occurs in sealed chambers heated to a predefined temperature in the absence of oxygen, creating an inert environment with limited gas passage. This method is highly effective in converting biomass into biofuel material. Pyrolysis involves the thermal

decomposition of biomass, releasing volatile and semi-volatile materials. At high temperatures, the mass decomposes, producing bio-oil and biochar[31,54].

Various technologies currently exist for activated carbon production, including biomass pyrolysis methods such as slow, fast, torrefaction, or gasification. The choice of the production method plays a crucial role in yield and final properties[55]. Slow pyrolysis, in particular, yields higher efficiency compared to other techniques[56,57].

2.3.1.1.1. Activated carbon

Activated carbon (AC) is a carbon-rich material resulting from the thermal conversion of biomass. It is widely used to enhance environmental quality, whether in removing pollutants from liquid or gaseous mediums, long-term carbon storage, or soil improvement[58,59]. Producing activated carbon from low-cost precursors has garnered significant interest among researchers due to its economic and environmental benefits[60].

The material can be employed to remove color, odor, taste, organic and inorganic substances, and pollutants in wastewater treatment. It is also utilized in air purification and the chemical, pharmaceutical, and food industries[61–63]. Despite being considered a costly adsorbent, given the relationship between quality and production cost, its high adsorption capacity compared to other fundamental adsorbents renders it an essential component, even with higher costs[64]. Various carbonaceous materials can be used in activated carbon production, including babassu[65], peach pit shells[66], brewery residues, coffee husks[67], and olive pomace[67].

AC has various applications, including its use as a food additive or composting agent in livestock farming and in the construction sector, where it aids in foundation decontamination and reduction of electromagnetic radiation[44]. Additionally, it is employed in soil as part of sustainable practices to enhance agricultural productivity, promoting plant root development and aiding in climate change mitigation[68–70].

The adsorption of organic compounds using activated carbon is a widely employed technology in treating and purifying wastewater and industrial waters. This application is attributed to its ability to remove metals, organic substances, odor, and color, acting as an adsorbent in water and wastewater treatment[71–73]. AC has specific characteristics, such as its internal surface area (800 to 1,200 m^2/g) and high porosity, enabling efficient adsorption of molecules in liquid and gaseous mediums[74,75]. Its high adsorption capacity makes it ideal for removing contaminants in aqueous environments, eliminating organic compounds, and purifying wastewater[74,76]. The properties of AC vary based on different factors, such as biomass selection, reaction temperature, and heating rate, among others[54]. Due to its microporous, mesoporous, and

macroporous structure, activated carbon stands out as an effective adsorbent[77].

Regarding pore size, the classification of pore levels in activated carbons, according to adsorption properties established by the International Union of Pure and Applied Chemistry (IUPAC), is detailed in Table 4.

Table 4 - Pore Classification According to IUPAC[78]

Type of Pores	Diameter (nm)
Micropores	< 2
Mesopores	2 – 50
Macropores	> 50

According to IUPAC[78], micropores constitute the majority of the surface area, providing a high adsorption capacity for molecules with dimensions smaller than 2 nm, including common gases and solvents. Mesopores, ranging in diameter from 2 to 50 nm, are distinguished by their larger sizes and their ability to adsorb large molecules, such as dyes and chemicals that can be impregnated into activated carbon. Although typically considered insignificant for adsorption, macropores (with a diameter greater than 50 nm) can serve as a means of transport for gaseous molecules. In this study, the activated carbon was activated using a greenhouse gas, specifically carbon dioxide (CO_2).

2.3.1.2. Wastewater Treatment Systems of the Olive Pomace Oil Extraction Industry

Wastewater treatment systems are classified as a basic sanitation measure aimed at expediting the water purification processes before discharge into the natural environment[40]. Various treatments are employed to mitigate the harmful effects of turbid waters on the environment, with primary approaches encompassing physical, chemical, and biological methods. These methods can be integrated with other methodologies[21,79,80], membrane filtration[81,82], advanced chemical oxidation (Fenton reaction)[38,83], adsorption using activated carbon[84,85], anaerobic[86], and aerobic digestion[87,88].

As common wastewater treatment stages depend on the characteristics of the wastewater and can encompass four treatment phases: preliminary treatment, primary treatment, secondary treatment, and tertiary treatment[89,90]. Preliminary or pre-treatment solely involves physical-chemical processes specifically designed to remove coarse pollutants. This stage includes the removal of floating debris through methods such as screening, sand traps, flotation units,

settling tanks, and filters[34]. Primary treatments involve additional physical-chemical processes, including pre-aeration, flow equalization, and wastewater load neutralization in an equalization tank. Subsequently, liquid and solid particles are separated, allowing the removal of colloidal material, color, turbidity, acids, alkalis, heavy metals, and oils through processes like flocculation, coagulation, primary settling, and precipitation[33,90,91].

In turn, the secondary treatment comprises biological processes followed by physical-chemical processes. Biological wastewater treatment processes involve the removal of biodegradable organic pollutants and can occur through aerobic or anaerobic systems. Utilizing intensive systems based on natural self-purification phenomena, this method employs reactors designed to create a favorable environment for microorganisms to degrade organic matter. Mechanical aeration is employed to supply oxygen for this process[34,92].

Tertiary treatment also involves physical-chemical processes, focusing on removing pathogenic microorganisms through maturation ponds and nitrification. This treatment phase is recognized for employing advanced methods to enhance the disinfection process, utilizing contaminant removal techniques such as chemical oxidation, ultraviolet radiation, ozonation, membranes, and activated carbon[21,33]. The conventional wastewater treatment process is illustrated in Figure 3[92,93].

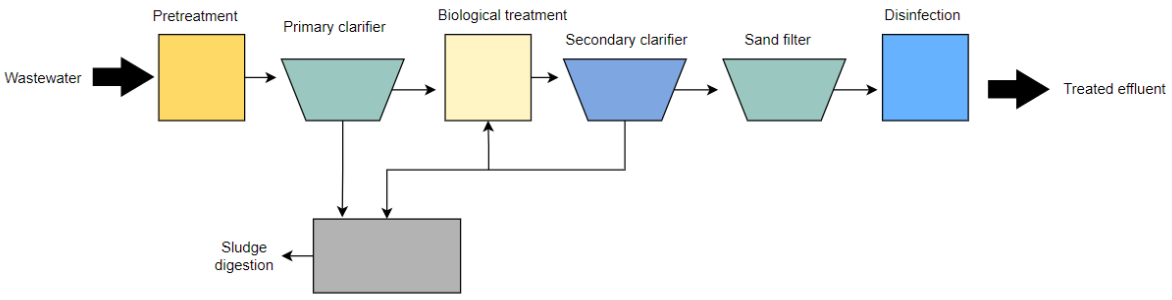

Figure 3 - Flowchart of the conventional effluent treatment process.

2.3.1.2.1. Membrane Utilization in Wastewater Treatment

Currently, the application of various membrane types (such as microfiltration, ultrafiltration, nanofiltration, and reverse osmosis) in water treatment has become essential for the efficient recovery of this resource, owning to the membranes' ability to remove microbiological contaminants, dissolved ions, and heavy metals[94]. This method offers numerous advantages, including selective separation, low energy consumption, ease of application, resource recovery, operation at low temperatures, requiring less space, and eliminating the need for chemicals, making it highly effective in treating wastewater, domestic, and brackish water sources[93,95].

Polymeric membranes, in particular, stand out due to their capacity to be integrated into other separation processes[96]. For this reason, they are often employed in combination with other technologies, as illustrated in Figure 4. In this context, they replace conventional steps such as secondary clarifiers, sand filters, and disinfection, providing benefits such as reducing the number of treatment stages, enhancing organic matter removal, and minimizing solid waste production during the treatment process[39].

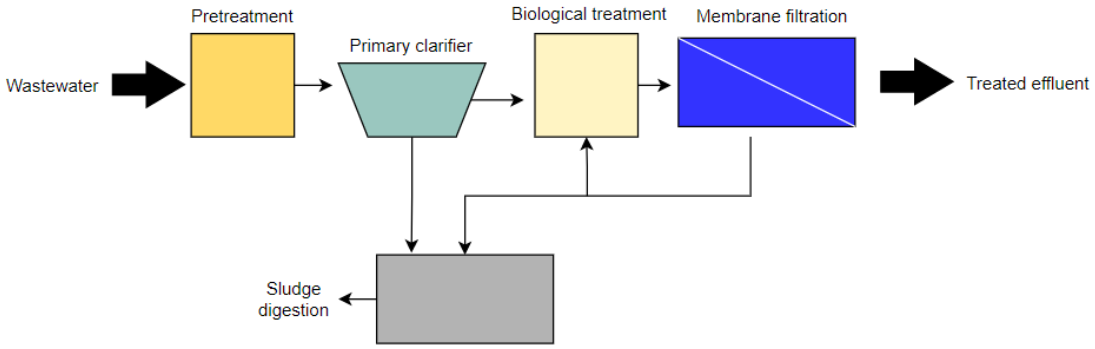

Figure 4 - Flowchart of the wastewater treatment process with membrane filtration.

As Membranes can be produced from various polymeric precursors, which are responsible for pore development. The methodologies employed in membrane production include techniques such as phase inversion, synthesis, and stretching. However, methods like solvent evaporation, extrusion, lamination, blowing, and phase inversion applied to microporous support are utilized to fabricate dense membranes. These techniques may involve processes like spreading, natural polymerization, or plasma[97,98]. It is crucial to evaluate several characteristics of polymeric membranes, such as filtration capacity, chemical resistance, water absorption, density, porosity, membrane morphology, and water permeability testing[97].

The use of membranes in wastewater treatment systems has increased over the years due to their recognition as an effective practice for removing dissolved pollutants in wastewater, especially those challenging to remove by other methods. Moreover, membranes offer the advantage of compactness, reducing the space requirements for water treatment plants[80,81]. Examples of such approaches include membrane filtration[81,82] and adsorption using activated carbon[84,85], which contribute to even more effective purification of this wastewater before its discharge into the natural environment. They represent an innovative and promising alternative for treatment and filtration, capable of retaining biomass through microfiltration, nanofiltration, ultrafiltration, and reverse osmosis[99].

2.4 Types of polymeric membranes

Microfiltration is widely employed in wastewater treatment, allowing for the retention of particles present in wastewater compared to traditional filtration methods[100]. This technique can retain turbidity, pathogens, fine colloidal particles, and microorganisms using a microfiltration membrane (MF) and a pressure rate[101]. The MF can filter particles as small as 0.1 micrometers (μm); however, the pressure applied in the process is directly related to the membrane's retention capacity, varying up to 10 μm in retention. This relationship between pressure and the diameter of the retained particle is proportional, as higher pressure applied to the water flow makes particle passage more accessible, allowing them to pass through the membrane pores[102]. The MF system is often used as a pre-treatment for ultrafiltration and nofiltration, and processes utilizing reverse osmosis membranes, as it does not eliminate microscopic pollutants due to the larger pore size[82]. With the advancement of the industry, membranes are produced from different materials, with polymers being the most commonly used.

Previous studies[103] investigated the efficiency of the MF system coupled with a coagulation/flocculation technique for removing polyphenol blue dye, which is widely used in textile industries for dyeing purposes. The catalyst used in the membrane was TiO_2, enabling the reduction of particles embedded in the membrane. The study concluded that by utilizing the coagulation/flocculation system, followed by the application of MF with TiO_2, there was a 100% removal of the dye and a decrease in the particle retention rate in the membrane.

Ultrafiltration (UF) is similar to the microfiltration system; however, the distinction between the two lies in the pore size of the membrane, which can be 10 times smaller, enabling a more specific filtration and allowing the retention of high molecular weight particles[104]. In the UF process, the solution is forced against the membrane (Pumping), allowing the passage to permeate and removing suspended solids, bacteria, viruses, and other pathogens. Solids with larger diameters tend to accumulate on the membrane surface, separating retained material and permeate[105].

In a study conducted by Bhattacharya[104], a membrane adsorption system coupled with nanoparticles was employed to remove ibuprofen from water treatment processes. The removal efficiency of the process was enhanced by utilizing a ceramic ultrafiltration membrane coated with zinc oxide (ZnO) nanoparticles, aiding in the removal of atenolol and ibuprofen from the solution. Consequently, the study demonstrated an impressive removal rate of 96% for atenolol and 99% for ibuprofen using a single-stage UF system.

Nanofiltration (NF) operates in conjunction with a pressure-driven system[82], effectively

removing divalent ions from saline water and reducing water hardness during purification[106]. This method provides several advantages, including low-pressure operation, cost-effectiveness, and high separation efficiency for organic molecules. However, it has limitations such as high energy consumption and the requirement for pre-treatment[107]. NF becomes more advantageous when integrated into a series of membrane systems, enabling the removal of color, heavy metals, and desalination.

In a study conducted by Roy[108], the production of composite ceramic-supported CSP nanofiltration membranes was enhanced by incorporating copper ions on the surface. Different concentrations of copper chloride solution were applied to the membrane surface to assess its performance in removing cationic and anionic heavy metals Ni, Cd, Pb, Zn, and Cr from the aqueous solution. The study yielded a removal rate of over 95% for all heavy metals.

Reverse Osmosis (RO) membranes have significantly smaller pores than other membranes, allowing for more effective retention of organic and inorganic particles, thereby enhancing the filtration system[109]. This technique is characterized by the flow of water from the more concentrated medium to the less concentrated one. Due to its smaller pores, it can retain minerals, dissolved particles, monovalent ions, and harmful substances, ensuring the passage of purified water[110]. The filtration efficiency relies on a gentle and continuous flow regulated by the pressure applied to the membrane, and requires pre-filtration to extend the membrane's lifespan and prevent early saturation[82].

A polymeric membrane can encompass various approaches, preparation methods, and characterization techniques. Yet, all membranes are composed of polymeric materials, such as polyethersulfone (PES)[111], polyacrylonitrile (PAN)[112], polypropylene (PP)[113], polysulfide (PS), polytetrafluoroethylene (PTFE), polyvinylidene fluoride (PVDF), among other polymers. PVDF is a semicrystalline polymer that exhibits solvent resistance. Its chemical resistance to many acids and alkalis imparts thermal stability. At the same time, its amorphous phase provides the flexibility desired in a membrane[114].

PVDF is also renowned for its hydrophobic properties, enabling an effective barrier against the passage of liquid contaminants. Its mechanical attributes ensure the structural stability of the membrane during the filtration process, enhancing the material's durability and lifespan[99]. However, the high hydrophobicity also poses a drawback. Nevertheless, a method that aids the membrane in reducing its hydrophobic character involves grafting hydrophilic polymers onto the hydrophobic surface of the membrane. This approach aims to enhance the membranes interaction capacity with organic compounds and other polar substances in the wastewater[115–117].

Polyvinylpyrrolidone (PVP) is hydrophilic, facilitating interactions with water molecules and aqueous solutes, aiding in enhanced adsorption and retention of organic contaminants[118]. Incorporating PVP into membrane production seeks to optimize its water affinity, similar to its ability to retain pollutants in the wastewater[119].

3. OBJECTIVES

Develop polymeric membranes utilizing activated carbon derived from EOP generated by the OPOEI. Evaluate the effectiveness of these membranes in a wastewater treatment model featuring contaminants such as phenol as a representative of phenolic compounds.

3.1 Specific Objectives

- Produce pyrolyzed AC-CO_2 from extracted olive pomace with enhanced porosity through the process of physical activation using CO_2;
- Characterize the physical and chemical properties of the produced AC-CO_2;
- Develop polymeric membranes using PVDF, PVP and NMP as a base material, incorporating the synthesized AC-CO_2;
- Conduct a comprehensive characterization of the polymeric membranes to assess their structural, morphological, and functional properties;
- Development of a surface analysis to study for the optimal ratio of the polymeric precursosrs in the synthesis of the polymer membranes;
- Evaluate the application of the developed polymeric membranes in filtration and adsorption processes targeting the removal of phenol from wastewater.

4. MATERIALS AND METHODS

4.1 Reactants and equipaments

4.1.1 Reactants

- Carbon Dioxide (CO_2), provided by Air Liquide;
- Distilled water;
- Hydrochloric acid 37% (HCl), provided by AnalaR Normapur;
- NMP - 1-Methyl-2-pyrrolidone (C_5H_9NO) provided by Thermo Scientific;
- EOP - Olive pomace, provided by Mirabaga - Food Industry and Commerce S.A;
- Phenol crystallized (C_6H_6O), provided by Panreac;
- PVDF - Polyvinylidene fluoride($-CH_2CF_2-)_n$, provided by Thermo Scientific;
- PVP - Polyvinylpyrrolidone $(C_6H_9NO)_n$, provided by Thermo Scientific;
- Sodium chloride (NaOH - 98%), provided by Labkem.

4.1.2 Equipaments

- HPLC;
- Knife film applicator;
- Magnetic stirrer;
- pHmeter;
- Pyrolysis oven;
- Sieves.

4.2 Methods

4.2.1 Production of Activated Carbon and Polymeric Membrane

4.2.1.1 Synthesis of Activated Carbon (AC_CO_2)

Activated carbon is produced by slow pyrolysis in an inert atmosphere created by circulating a N_2 flow of 100 N mL min^{-1}. The heating ramp for AC_CO_2 production, as shown in Figure 5, includes an initial 2 hour conditioning period with nitrogen injection. Porosity is then slowly developed over 8 hours, with the heating ramp initiated from the third hour onwards, gradually increasing the temperature at a rate of 5°C per minute. When 800°C is reached, CO_2 injection is carried out for 1 hour to induce an increase in porosity formation. The nitrogen flow is resumed until the production process is complete.

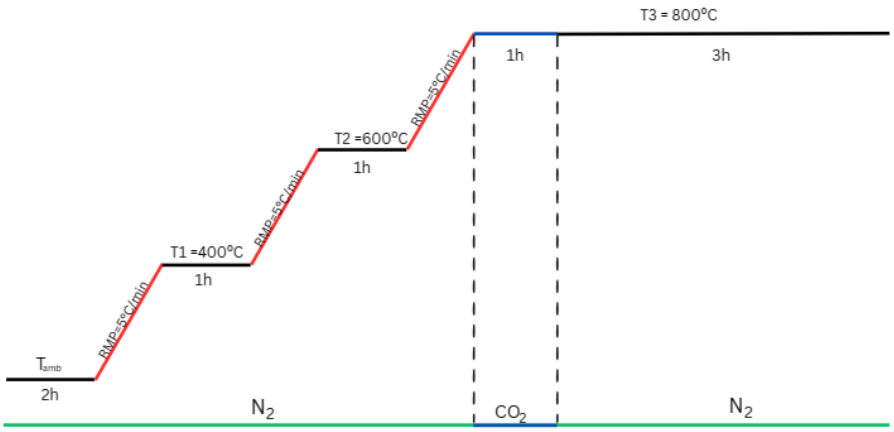

Figure 5 - Scheme of the slow pyrolysis process for the production and activation of carbon

After cooling the pyrolysis oven under a nitrogen atmosphere, the material is removed and screened in order to obtain a particle size of less than 53 µm.

4.2.1.2 Preparation of Polymeric Membranes

4.2.1.2.1 Experimental Design

The response surface method (RSM), was developed to optimize laboratory analyses for membrane production, encompassing a range of mathematical and statistical techniques for building empirical models and exploring the model[130]. Through appropriate experimental planning and analysis, the RSM seeks to relate a response to the levels of a series of input variables or factors that influence it. In this study, the Box-Behnken design (BBD) was chosen to investigate and associate three independent parameters: PVP, NMP, and PVDF. This method establishes the relationship between these independent variables using second-order polynomial equations (Eq. 1).

$$Y = \beta_0 + \sum_{i=1}^{k} \beta_i X_i + \sum_{i=1}^{k=1} \beta_{ii} x_i^2 + \sum_{i<j} \sum_{j}^{k} \beta_{ij} X_i X_j \qquad (1)$$

In the above equation, Y represents the output response, while x corresponds to the independent variables affecting this response. The values of "β" are equivalent to the regression coefficients for the intercept (β0), linear terms (βi), quadratic terms (βii), and interactions (βij). Additionally, "k" represents the number of variables in the system.

Box and Behnken introduced an experimental design involving three levels for constructing response surfaces. These experiments are created by combining factorial experiments with

incomplete block designs, either rotational or nearly rotational[131]. The BBD excludes points at the vertices formed by each variable's upper and lower bounds. This approach can be beneficial when the points at the corners of the cube represent combinations of factor levels that are challenging or impossible to test due to physical constraints (Figure 6).

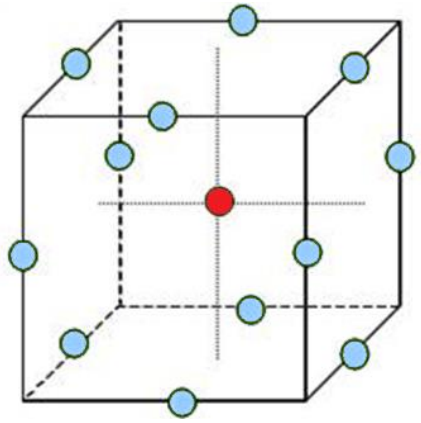

Figure 6 - BBD for 3 independent variables

Table 5 presents the intervals and experimental values of the independent variables considered for the project, which were determined based on the collection of experimental data available in the literature.

Table 5 - Experimental variables and their levels used in the BBD.

Factor	**Original Factor**	**Levels**		
		-1	**0**	**1**
PVP	X1	1	7	13
PVDF	X2	3	11.5	20
NMP	X3	72	80	88

The design was planned and created using R-Studio software, where the design concept, mathematical modeling, graphical and statistical treatment of the results, and optimization were developed. The recorded response values for membrane fabrication are presented in Table 6.

.

Table 6 - Box–Behnken design layout

Experiment Logical	Coded Factors		
	X1	X2	X3
1	-1	-1	0
2	1	-1	0
3	-1	1	0
4	1	1	0
5	-1	0	-1
6	1	0	-1
7	-1	0	1
8	1	0	1
9	0	-1	-1
10	0	1	-1
11	0	-1	1
12	0	1	1
13	0	0	0
14	0	0	0
15	0	0	0

4.2.1.2.2 Production of Polymeric Membranes

The BBD method was employed to develop mixed matrix polymeric membranes incorporating the produced activated carbon, with the activated carbon value included as a fixed variable in the experiment. Fifteen polymeric membranes were manufactured, and the details of each sample, including the exact quantity of each component in every developed test, are presented in Table 7.

Table 7 - The quantity of reagents for the formulation of polymeric membranes incorporating activated carbon.

Experiment		PVP (g)	PVDF (g)	NMP (g)	AC_CO_2
Logical	**Random**				
1	2	1.3	0.3	8	2.5
2	14	0.7	1.15	8	2.5
3	6	1.3	1.15	7.2	2.5
4	15	0.7	1.15	8	2.5
5	1	0.1	0.3	8	2.5
6	5	0.1	1.15	7.2	2.5
7	7	0.1	1.15	8.8	2.5
8	3	0.1	2	8	2.5
9	12	0.7	2	8.8	2.5
10	13	0.7	1.15	8	2.5
11	8	1.3	1.15	8.8	2.5
12	4	1.3	2	8	2.5
13	10	0.7	2	7.2	2.5
14	9	0.7	0.3	7.2	2.5
15	11	0.7	0.3	8.8	2.5

Using the BBD method incorporating AC_CO_2, each sample was subjected to ultrasound for 3 hours to achieve a homogeneous mixture. Subsequently, PVDF was added to the resulting gel, which was then placed in an agitated bath at 40°C, 200 rpm, for 48 hours. This procedure enabled the formation of polymeric membranes with controlled incorporation of AC_CO_2, ensuring a uniform distribution of the material and providing desirable characteristics for its application.

After 48 hours, the material needed to rest for at least 12 hours. After this resting period, the material was spread using the Knife film applicator equipment at thicknesses of 150 µm, 200 µm, and 300 µm. Following the material spreading, the gel was immersed in a coagulation bath of distilled water. This process can be analyzed through the schematic diagram depicted in Figure 7.

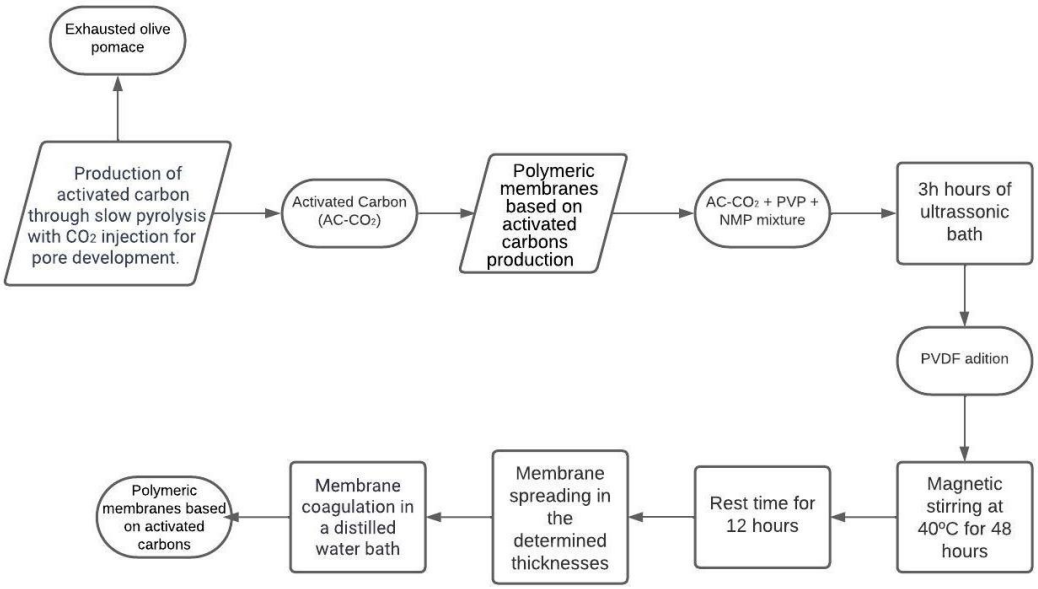

Figure 7 - Schematic diagram for membrane preparation

4.2.2 Characterization of Materials

4.2.2.1 Elemental analysis (CHNS)

Elemental analysis CHNS is important for determining the levels of carbon (C), hydrogen (H), sulfur (S), and nitrogen (N). The technique is characterized as a method based on the complete oxidation of the sample by combustion and the analysis of the released gases. The elemental composition in the solid and oily phases was determined using a CHNS Flash 2000 analyzer (Thermo Fisher Scientific, Massachusetts, USA), equipped with a thermal conductivity detector (TCD). C, H, S, and N contents were determined by an oxidation/reduction reactor maintained at a temperature of 900°C.

4.2.2.2 Ash Content

The ash content describes the mineral and inorganic material in activated carbon. It is typically determined by crushing and heating the material at high temperatures, where volatile components are removed. The ash determination method involves weighing the sample and subjecting it to combustion in a muffle furnace at 800°C for 1 hour in an uncontrolled atmosphere. When no organic matter residue is left in the sample, the ash is ready to be removed from the muffle furnace. It is then transferred to a desiccator to cool and weighed as soon as it reaches room temperature. The ash percentage is calculated by comparing the material's initial mass with the remaining material's mass (Eq. 2).

$$\text{Ash content (\%)} = \frac{\text{mass of initial sample} - \text{mass of ash residue}}{\text{mass of the sample}} \text{ x } 100 \qquad (2)$$

4.2.2.3 pH Point of Zero Charge (pzc) Determination

In Erlenmeyer flasks, nine dilutions of 0.01 mol/L NaCl were prepared. The pH of each solution was adjusted to values between 4 and 12 by adding 0.02 mol/L NaOH or HCl. To study the effect of pH on the performance of the material as an adsorbent (AC_CO_2), 0.15 g of the solid sample was added to each solution, which was then stirred on a magnetic stirrer at 300 rpm and 25ºC for 24 h. After filtering the solutions, their pH was measured. The final pH values were plotted on the y-axis and the corresponding initial values on the x-axis. A correlation was established between these two values and an identity curve was plotted on the graph. The point of intersection between the pH curves and the identity curve represents the pH at the point of zero charge (pHpzc).

4.2.2.4 Acid-Base Characterization

The content and type of oxygenated groups present in it determine the acidity and basicity of a material. Identifying these groups can significantly impact the performance of AC_CO_2 as adsorbents[9,10]. Furthermore, this analysis allows the investigation of interaction mechanisms between the adsorbate and the adsorbent, providing detailed information about surface charge. To assess this property, five different solutions were prepared:

- 1 L of NaCl 0.01 mol L^{-1}
- 500 mL of HCl 0.02 mol L^{-1}
- 500 mL of HCl 0.01 mol L^{-1}
- 500 mL of NaOH 0.02 mol L^{-1}
- 500 mL of NaOH 0.01 mol L^{-1}

Titration enables the determination of the concentration of a titrated solution based on its known concentration and volume. When this method is applied to AC_CO_2, it becomes possible to calculate the number of moles that react with the acidic or basic sites present in the material. This procedure provides valuable information about the acid-base properties of the material, allowing the characterization of its acidity or basicity.

To determine the material's acidity, 0.2g of the material was added to 25 mL of a 0.02 mol L^{-1} NaOH solution. The mixture was stirred on a magnetic stirrer at 600 rpm for 48 hours. The resulting solution was then filtered, and an aliquot of 20 mL of the recovered solution was titrated with a 0.01 mol L^{-1} HCl solution, using phenolphthalein as an indicator.

To assess the basicity, 0.2g of the sample was added to 25 mL of a 0.02 mol L^{-1} HCl solution.

The mixture was stirred on a magnetic stirrer at 600 rpm for 48 hours. After filtration, 20 mL of the recovered solution was titrated with a 0.01 mol L^{-1} NaOH solution, and phenolphthalein was used as an indicator.

4.2.2.5 Porosimetry and surface area

The surface area is a critical information in AC_CO_2, directly influencing their adsorption capacity. The most common method used to measure surface area is the Brunauer-Emmett-Teller (BET) method. The Quantachrome NOVA TOUCH LX4 equipment was used to measure the adsorption-desorption isotherms of liquid nitrogen at 77 K as a function of pressure. The out-gassing process was executed at 200°C for 3 hours, and the BET equation was applied using the Quantachrome Touch Win software within the range of p/p0 from 0.05 to 0.35 to estimate the surface area.

4.2.2.6 Determination of Surface Chemistry

The surface functional groups of the AC_CO_2 were estimated by Fourier Transform Infrared (FTIR) spectroscopy analysis (Perkin Elmer FT-IR, spectrophotometer UATR). FTIR spectra of different samples were recorded in the range of 450 - 4000 cm^{-1}. The transmission spectra of the samples were recorded using a KBr pellet. Approximately 1.0 - 2.0% of the sample was mixed with dry KBr and ground in a mortar. The mixture was then transferred to a hydraulic press. The pressure in the hydraulic pump was increased to 80 tonnes and then gradually released. The resulting pellet, which had a homogeneous and transparent appearance, was placed in the FTIR sample holder for analysis. The raw data was subjected to Fourier transformation to produce the actual spectrum for subsequent analysis.

4.2.2.7 Thermogravimetric Analysis

The thermogravimetric analysis (TGA) method records a specific sample's mass loss as a temperature function. The method essentially involves analyzing key parameters: mass, temperature, and time. Thermogravimetric curves will be obtained using the TA Instruments TGA SDT650 equipment, with a 100 mL min^{-1} air or N_2 atmosphere flow rate, a 10 °C min^{-1} heating ramp from 40 to 900 °C, and an open ceramic crucible.

4.2.2.8 Morphological Analysis

The scanning electron microscopy (SEM) was carried out to study the morphological and microstructural characteristics of polymeric membranes with and without activated carbon. This analysis was carried out at the University of Trás-os-Montes e Alto Douro.

4.2.3 Analysis and Application Methods

4.2.3.1 Kinetics and adsorption isotherms with AC_CO_2

A series of procedures were performed to evaluate the adsorption kinetics of the AC_CO_2 for phenol. Batch adsorption experiments were conducted for phenol adsorption on the produced activated carbon. A stock solution of 100 mg L^{-1} of phenol was prepared and diluted as needed to obtain different phenol solution concentrations (75 mg L^{-1}, 50 mg L^{-1}, 30 mg L^{-1}, 15 mg L^{-1}). For the analysis, 10 mL containers were used, with 0.025g of activated carbons added to each container, resulting in a concentration of 2.5 g L^{-1} of adsorbent. All experiments were carried out at room temperature (23°C) on a magnetic stirrer plate with a constant stirring speed of 600 rpm for 48 hours, with samples collected at 8, 24, and 48 hours, at the end of each collection, the sample was vacuum-filtered to separate the adsorbent from the solution, the determination of phenol was performed using high-performance liquid chromatography at 277 nm. The adsorption capacity q (mg/g) was determined using Eq. 3, while the removal efficiency of AC_CO_2, E (%), was calculated using Eq. 4.

$$q = \frac{(C_0 - C_e)x\,V}{m} \quad (3)$$

$$E = \frac{C_0 - C_e}{C_0}\ x\ 100\% \quad (4)$$

Where C_0 (mg L^{-1}) is the initial concentration of the pollutant (phenol), Ce (mg L^{-1}) indicates the concentration of the pollutant in the liquid phase at equilibrium, V (L) stands for the volume of the pollutant solution, and m (g) represents the mass of the adsorbent.

The graphs can take various forms, providing valuable insights into adsorption, as illustrated in Figure 8.

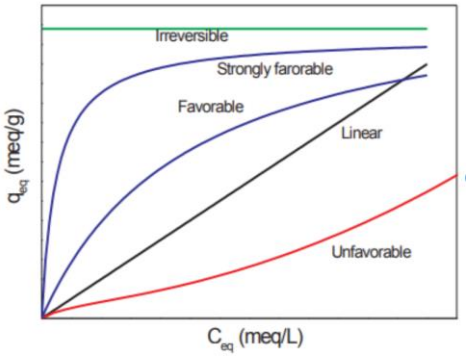

Figure 8 - Adsorption isotherms[123]

4.2.3.1.1 Kinetic models

Adsorption equilibrium studies are critical to determine the effectiveness of the process and are also crucial to study the nature of the adsorption mechanism. The purpose of this analysis is to explore the adsorption mechanism and provide important information on the interactions between adsorbent and adsorbate and on the various phases of the process, including mass transfer of the adsorbent material and chemical interactions at the liquid-solid interface[124]. Several solid-liquid adsorption kinetic models have been proposed. This study was performed using pseudo-first-order, pseudo-second-order, and intra-particle diffusion models (Eq. 5,6 and 7).

Pseudo-first order model	$\mathrm{qt} = \mathrm{qe}(1 - e^{-k_1 t})$	(5)
Pseudo-second order model	$\mathrm{qt} = \frac{q_e^2 k_2 t}{1 + q_e^2 k_2 t}$	(6)
Intra-particle diffusion	$\mathrm{q} = \mathrm{k_{id}} \mathrm{t}^{1/2} + \mathrm{I}$	(7)

Where q_t t is the adsorption capacity (mg.g^{-1}) at a time t (min), q_e is the adsorption capacity at equilibrium (mg g^{-1}), and k_1 is the adsorption rate kinetic constant of the pseudo-first-order model (min^{-1}), k_2 is the adsorption rate kinetic constant of the pseudo-second-order model (g mg^{-1} min^{-1}), k_{id} is the intraparticle diffusion rate constant (mg (g·min$^{0.5}$)$^{-1}$), and I (mg g^{-1}) is the intercept.

4.2.3.1.2 Equilibrium isotherms

To construct the equilibrium isotherms, it was necessary to prepare a 10 mL solution of phenol with five different concentrations: 15, 30, 50, 75, and 100 mg L^{-1}. 0.025 g of AC_CO_2 were added to the solution, resulting in a concentration of 2.5 g L^{-1} of adsorbent. The solutions were stirred at 600 rpm at a temperature of 23°C for 48 hours. Samples were collected after 8, 24, and 48 hours from the start of the analysis. After collection, the samples were vacuum-filtered to separate the adsorbent from the solution, and the phenol concentration was determined using HPLC at 277nm.

4.2.3.1.2.1 Equilibrium isotherms models

The isotherms of adsorption are essential for studying the equilibrium relationship between a solute adsorbed on the surface of AC_CO_2 and the adsorbed solute in the solution. They indicate the adsorption equilibrium stage, which is crucial for analyzing whether the adsorbent

material is suitable and exhibits favorable performance in the adsorption system[125]. Adsorption equilibrium is reached when there is no longer a perceptible variation in solute concentrations in the solution.

Some mathematical models are available to effectively capture and represent experimental equilibrium data, often visualized through isotherms. This study will employ the widely recognized Langmuir and Freundlich models to aptly fit and interpret the isotherm data, enhancing our understanding of the underlying processes[126,127].

The Langmuir isotherm proposes that adsorption occurs at a defined number of sites, each with equivalent energy, not exceeding monolayer coverage[128]. In other words, all surface sites are equivalent and can accommodate only one adsorbate molecule, where the adsorbed molecules do not interact. The molecule's capacity to adsorb at a specific site is independent of the occupation of neighboring sites.

The Langmuir model is represented by Eq. 8, where q is the concentration of the solute adsorbed on the solid surface ($mg.g^{-1}$), q_{max} is the maximum adsorption capacity ($mg.g^{-1}$), K_L is the interaction constant between adsorbate and adsorbent ($L.mg^{-1}$), and Ce is the solute concentration at equilibrium ($mg.L^{-1}$).

$$q = \frac{q_{max} \,.\, Kl \,.\, Ce}{1 + Kl \,.\, Ce} \tag{8}$$

Eq. 9 can be linearized, resulting in:

$$\frac{Ce}{q_e} = \frac{1}{k_L \, q_{max}} + \frac{1}{q_{max}} \, Ce \tag{9}$$

With this linearization, we can plot Ce/qe x Ce to obtain the desired parameters q_{max} and K_L.

The Freundlich isotherm model proposes that as the sites are occupied during adsorption, the energy with which the adsorbate interacts with the site decreases exponentially. This model describes non-ideal adsorption processes on a homogeneous surface with the formation of multilayers. Eq 10 represents the isotherm, where q ($mg\ g^{-1}$) represents the amount of adsorbate on the solid; Ce ($mg\ L^{-1}$) is the adsorbate concentration in the fluid at equilibrium, K_f represents the adsorption capacity, also known as the capacity factor ($(mg\ g^{-1}).(L\ mg^{-1})^{(1/n)}$), and n is the intensity factor of adsorption[129].

$$q = k_f \,.\, Ce^{1/n} \tag{10}$$

4.2.3.2 Filtration with Polymeric Membranes

A continuous model was employed to assess the effectiveness of the polymeric membranes in pollutant treatment, utilizing a reactor coupled with an HPLC pump (Figure 9). In the experiments, a pollutant, specifically phenol at a concentration of 50 mg L^{-1}, was placed in a

container with an inlet directly connected to the HPLC pump. The pump, operating at a flow rate of 0.5 mL min^{-1}, fed the pollutant through the reactor inlet and passed it through the polymeric membrane installed in the reactor. Samples (2 mL) were collected at intervals of 0, 5, 15, 30, 45, and 60 minutes during filtration. The treated wastewater was collected for subsequent analysis, allowing the evaluation of the membrane effectiveness in pollutant treatment.

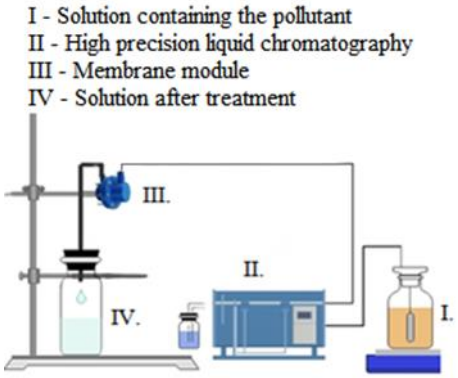

Figure 9 - Structural diagram for the membrane filtration system.

4.2.3.2.1 High Performance Liquid Chromatography (HPLC)

HPLC (high-performance liquid chromatography) was used to identify the presence of phenol in samples collected in the adsorption test (AC_CO_2) and filtration (Polymeric Membranes). The Ultra BiPh 5µm column (150 mm x 2.1 mm) was used for this analysis, along with a mobile phase comprising 50% of acetonitrile and 50% phosphoric acid + ultrapure water. The isocratic system was run at a flow rate of 0.3 $mL.min^{-1}$, and phenol was detected at a wavelength of 277 nm. Figure 10 presents a graphical representation of the calibration curve generated for the analyses.

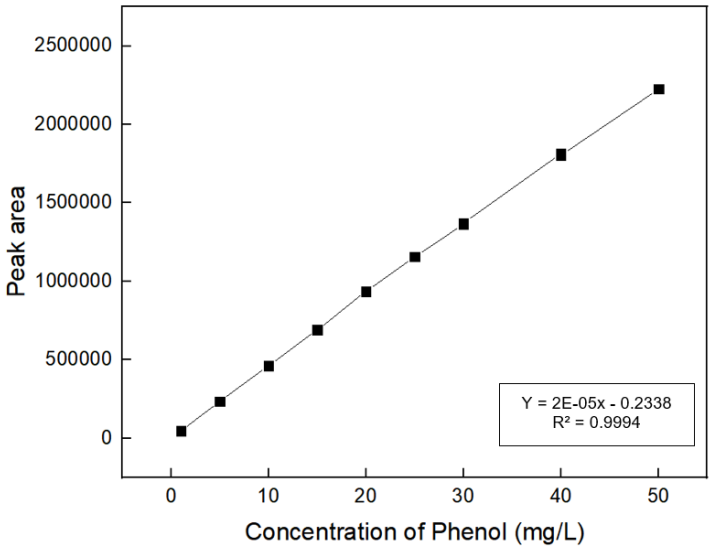

Figure 10 - Calibration curve for phenol measurements

Before analyzing the phenol solution obtained from the adsorption tests, a calibration curve was constructed within the 1-50 $mg.L^{-1}$ reading range. The calibration curve exhibited a high level of accuracy, as indicated by the excellent fit obtained with an R^2 value of 0,9994, determined through linear regression analysis

5. RESULTS AND DISCUSSION

5.1 Characterization of AC_CO_2

5.1.1 Elemental Analysis

The study employed EOP as a precursor for the production of AC_CO_2 due to its accessibility and abundance in the region, its potential for valorization as a waste material, and its widely distributed chemical composition. Table 8 presents the physical and chemical characterization of the materials. The influence of carbonisation on the final composition of AC_CO_2 is evident from the analysis of the carbon content, which increased from 49.1% in EOP to 62.65% in AC_CO_2 after the slow pyrolysis process. This justifies the transformative effects of carbonisation on the chemical composition of the materials. In contrast, the nitrogen and hydrogen contents decreased due to decarboxylation and dehydration reactions.

Table 8 - Elemental analysis of CNHS for EOP and AC-CO_2

(%)	**EOP**	**AC-CO_2**
Nitrogen	2	1.74
Carbon	49.1	62.65
Hydrogen	8	0.78
Sulfur	0.06	0
Ashes	4	17
Volatile Matter	40	16
Fixed Carbon	14	66

The proximal analysis indicates that the volatile matter content is higher in EOP than in AC-CO_2, which has a higher proportion of fixed carbon and ash in its composition. Conversely, EOP has only 14 % fixed carbon, while AC-CO_2 has 66 %. This is due to the lower presence of volatile components in AC-CO_2, resulting from the expulsion of volatile organic compounds during the carbonisation process, which leads to the formation of a porous carbon structure. These results from the analysis of C, N, H and ash content are consistent with similar investigations involving carbonisation processes initiated in EOP [134–136].

5.1.2 Adsorption Experiments

5.1.2.1 Kinetic models

The influence of the processing time on the adsorption capacity of the adsorbent (in $mg.g^{-1}$) was evaluated by studying the adsorption kinetics. The kinetic models presented in Eq. 5, 6

and 7 were fitted to the experimental data of adsorption kinetics. In addition, Table 9 presents the results obtained and Figure 11 shows the graphs describing the adjustments of the three kinetic models in relation to the experimental data evaluated for AC-CO_2 obtained in phenol adsorption.

Table 9 - Parameters of the kinetic models for the activated carbon.

Adsorbent	Pseudo-first-order				Pseudo-second-order			Intraparticle diffusion		
	q_{exp} (mg.g^{-1})	q_e (mg g^{-1})	K_1 (min^{-1})	R_1^2	q_e (mg g^{-1})	K_2 (g/mg.min)	R_2^2	I (mg g^{-1})	K_{id} (mg/g.$min^{1/2}$)	R_3^2
AC-CO_2	85.123	76.748	0.079	0.962	80.228	0.0018	0.986	33.884	2.717	0.636

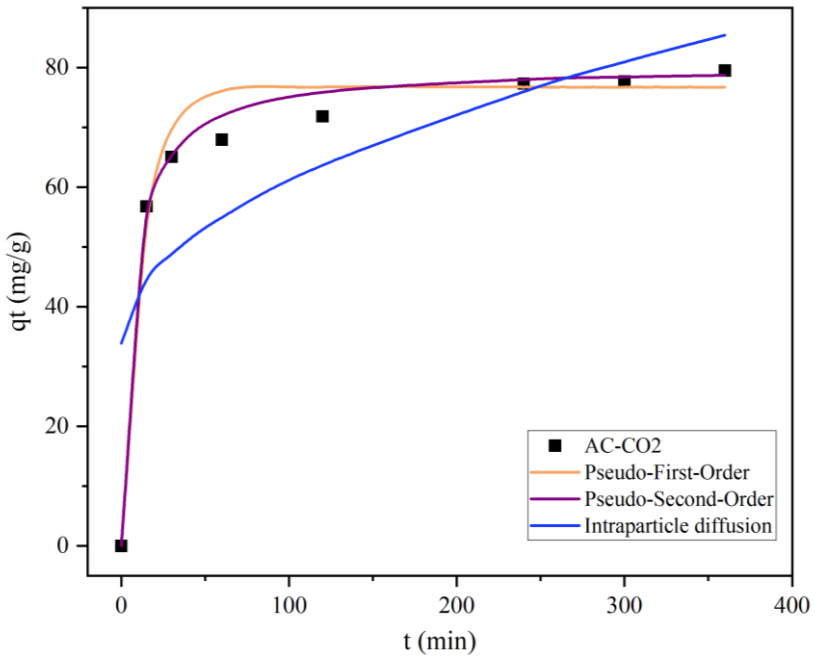

Figure 11 - Fitting the kinetic models to the experimental data for AC-CO_2.

Based on the results of the adsorption analysis presented in the previous chapter, it can be observed that the adsorption kinetics exhibited a higher initial adsorption rate, followed by a lower rate at a later stage. The graphical curves and R^2 values for AC-CO_2 were examined, and while the pseudo-first-order model yielded an acceptable R^2 of 0.96, it is worth noting that the pseudo-second-order model provided a superior fit with an R^2 of 0.99. According to the study, it was found that AC-CO_2 has an adsorption capacity of approximately 76 mg.g^{-1} for phenol. The pseudo-second-order model suggests that valence forces are formed through the exchange or shared use of electrons between the adsorbent and the adsorbate during adsorption[143,144]. It is worth noting that the intraparticle diffusion model had the lowest R^2 value for the material. It is worth noting that due to the complex and heterogeneous structures of carbonaceous adsorbents, interparticle diffusion may not always be a suitable model for these materials.

5.1.2.2 Equilibrium isotherms

The Langmuir and Freundlich models used to analyse equilibrium isotherms are referred to in Eq. 4, 5 and 6. The Langmuir isotherm assumes that the adsorbent surface has a finite number of active sites with uniform energy, and that adsorption is reversible. On the other hand, the Freundlich isotherm characterizes adsorption on heterogeneous surfaces. Table 10 presents the results, while Figure 12 illustrates the experimental values for adsorbed phenol (AC_CO_2) fitted to the Langmuir and Freundlich isotherm models.

Table 10 - Parameters of equilibrium models: Langmuir and Freundlich

Adsorbent	**Langmuir**			**Freundlich**		
	q_{max} (mg g^{-1})	**K_L (L.mg^{-1})**	**R^2**	**K_F (L.g^{-1})**	**n_F**	**R^2**
AC-CO_2	738.513	0.2262	0.817	234.625	43.916	0.979

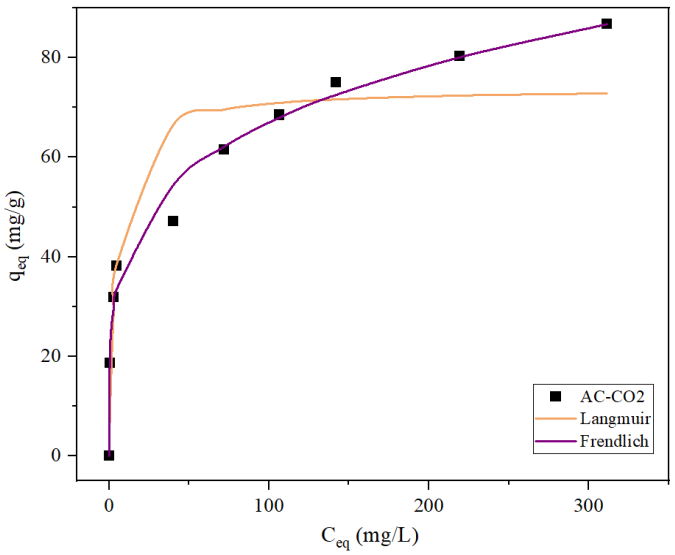

Figure 12 - Experimental results for phenol adsorption using the Langmuir and Freundlich isotherm models

The isotherm models were then applied to the experimental data, and it was found that the Freundlich isotherm model (R^2=0.979) was the most suitable fit. Therefore, this model can be used to represent the experimental data, describe the adsorption capacity, and determine the necessary quantities.

Paiva et al.[145,146] conducted research on the Freundlich equation, an empirical equation used to describe heterogeneous and reversible adsorption systems, which is not restricted to monolayer formation. According to their findings, the Langmuir isotherm is applicable to homogeneous adsorption systems, indicating that the adsorbent saturation has not yet been reached[146]. As a result, it is possible that the adsorption capacity may be even higher in a solution with a higher

initial concentration.

It is worth noting that while both models have their merits, the Freundlich model does not predict adsorbent saturation. As a result, the results obtained from the Freundlich model provide a good description of the equilibriums, which demonstrate the highest correlation coefficients.

5.2 Preparation and incorporation of polymeric membranes

5.2.1 Response surface analysis

During the development of the experiment, it was observed that only two of the polymer membranes met the established criteria for analysis, while the others exhibited deformities during the manufacturing process. The selection was based on fundamental characteristics such as resistance, adsorption capacity, and porosity, which are crucial for the performance and effectiveness of membranes in separation and purification processes (Table 11).

Table 11 - Response surface analysis

Experiment	**PVP (g)**	**PVDF (g)**	**NMP (g)**	**AC_CO_2**	**Observations**
1	0.1	0.3	8	2.5	Highly fluid consistency, lacks structural integrity
2	1.3	0.3	8	2.5	Formation of PVDF and AC_CO_2 aggregates, disintegrated upon coagulation.
3	0.1	2	8	2.5	Premature coagulation occurred
4	1.3	2	8	2.5	Rigid, limited malleability, exhibited cracking during stretching
5	0.1	1.15	7.2	2.5	Excessively thick consistency, experienced premature coagulation
6	1.3	1.15	7.2	2.5	Formation of PVDF and AC_CO_2 aggregates, resulting in a dense mass with low plasticity
7	0.1	1.15	8.8	2.5	Premature coagulation was observed

8	1.3	1.15	8.8	2.5	Successful outcome
9	0.7	0.3	7.2	2.5	Resulted in a liquid consistency
10	0.7	2	7.2	2.5	Premature coagulation was evident
11	0.7	0.3	8.8	2.5	Formation of aggregates, with insufficient resistance formed
12	0.7	2	8.8	2.5	Premature coagulation occurred
13	0.7	1.15	8	2.5	Successful outcome
14	0.7	1.15	8	2.5	Successful outcome
15	0.7	1.15	8	2.5	Successful outcome

It was observed that the selected membranes (Figure 13) for this study exhibited adequate mechanical strength to maintain their structural integrity during handling and operation. Furthermore, they exhibited a notable adsorption capacity, indicating the presence of active sites that are conducive to the removal of pollutants and unwanted solutes.

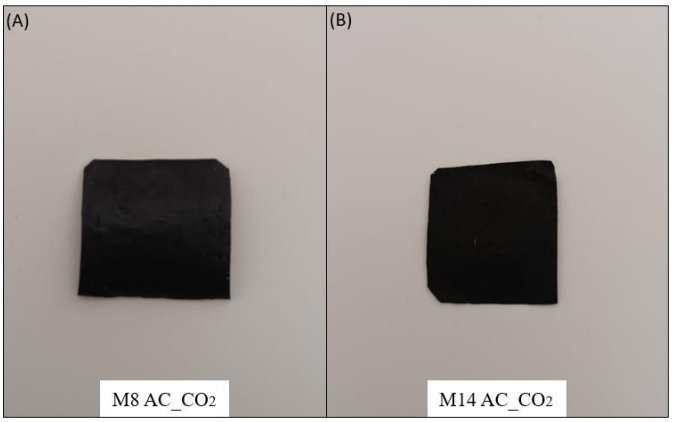

Figure 13 – Polymeric membrane of: a) formulation 8 with activated carbon; b) formulation 14 with activated carbon

However, it appears that the quality and performance of the other membranes may have been compromised due to deformations. It was determined that the precipitated coagulation that occurs during the manufacturing process is a significant contributing factor. This can be attributed to a formulation that contains a high amount of PVDF, which gives the membrane a hydrophobic character. It appears that the premature hardening of the solution during

manufacturing may have contributed to the production of a membrane with low resistance and susceptibility to damage, as can be observed in Figure 14.

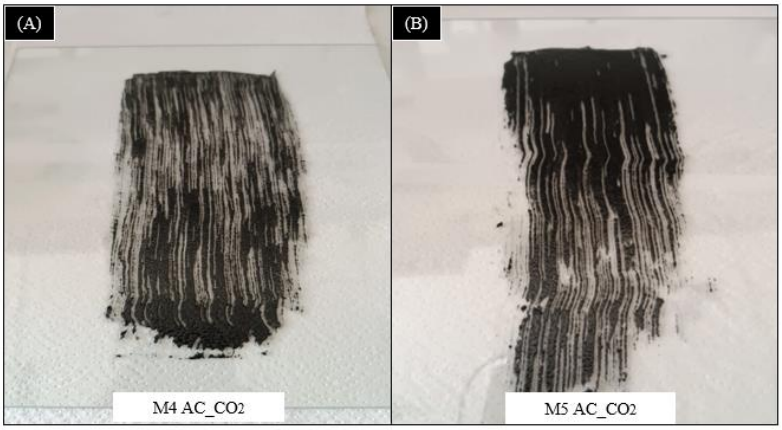

Figure 14 - Polymeric membrane of: a) formulation 4 with activated carbon; b) formulation 5 with activated carbon

Moreover, it seems that some membranes contained an excessive amount of PVP, which may have contributed to their hydrophobic character. This could potentially result in a weak interaction with aqueous materials and reduced resistance, thereby compromising the durability and effectiveness of the membranes in practical applications. This is illustrated in Figure 15.

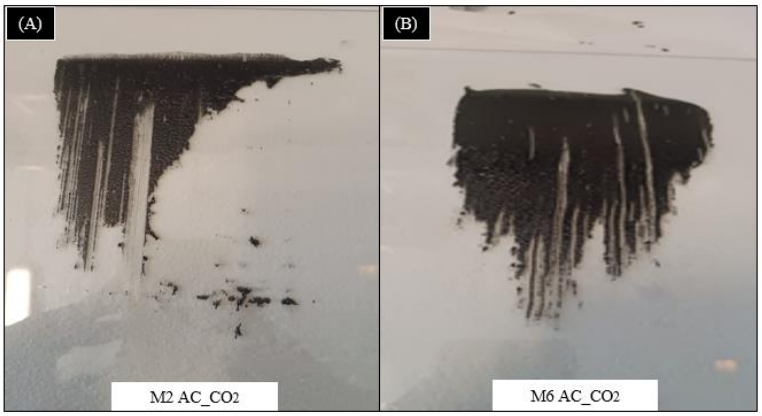

Figure 15 - Polymeric membrane of: a) formulation 2 with activated carbon; b) formulation 6 with activated carbon

The selection of two high-quality membranes (M8 and M14) was of paramount importance in ensuring the viability and quality of the results obtained during the experiment. The membranes meet the technical requirements and perform satisfactorily, which makes them promising for chemical and physical analyses. For the purpose of comparison, polymeric membranes were developed without the addition of activated carbon, with the objective of identifying the enhancements provided by the presence of AC_CO_2 in their composition. The development was conducted using formulations 8 and 14 of the experimental design, and Figure 16 illustrates the resulting membranes.

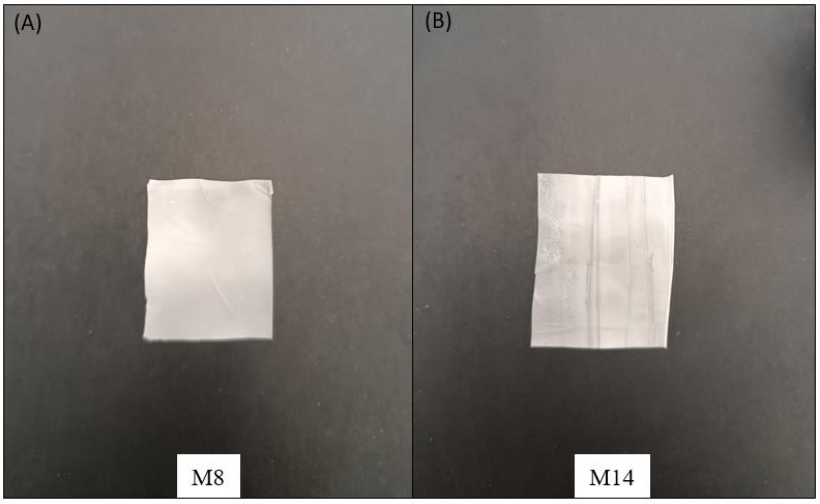

Figure 16 - Polymeric membrane of: a) formulation 8; b) formulation 14

5.3 Characterization of materials

5.3.1 Porosity Characterization

The Brunauer, Emmett, and Teller (BET) surface area analysis is a technique used to measure the specific surface area of samples. This analysis is crucial in producing materials with developed porosity, as surface properties are highly relevant for their application in wastewater treatment. The technique is based on gas adsorption to measure the surface area of the sample under analysis. Physical adsorption is a process that occurs due to the attraction between gas molecules and atoms present in the sample's composition. By exposing the sample to gas and measuring the amount of adsorbed gas, it is possible to determine the surface area of the sample. Table 12 depicts the Textural properties of EOP, AC-CO_2 and Polymeric Membranes.

Table 12 - Textural properties of EOP, AC-CO_2 and Polymeric Membranes.

Sample	S_{BET} ($m^2.g^{-1}$)	$S_{Langmuir}$ ($m^2.g^{-1}$)	S_{ext} ($m^2.g^{-1}$)	S_{mic} ($m^2.g^{-1}$)	V_{mic} ($mm^3.g^{-1}$)	W_{mic} (nm)
EOP	22	-	-	-	0.020	-
AC-CO_2	528	783	33	750	269	1.43
AC-CO_2 M8	7.71	247	7.71	0	0.05	0
AC-CO_2 M14	47.5	143	3.88	-	-	-
M8	2.32	355	2.33	-	-	-
M14	31	420,5	3.47	27.46	-	-

(-) not determined.

The analysis of the Sext, Vmic and Wmic parameters revealed the presence of pores of varying sizes, indicating the material's capacity to form mono and multisolvent layers. These

characteristics exemplify the versatility of AC-CO_2. Figure 17 illustrates the N_2 adsorption-desorption isotherms at 77 K for AC-CO_2. Furthermore, the surface area of AC-CO_2 is notably superior to those observed in alternative activation methods in other studies related to EOP[2,3].

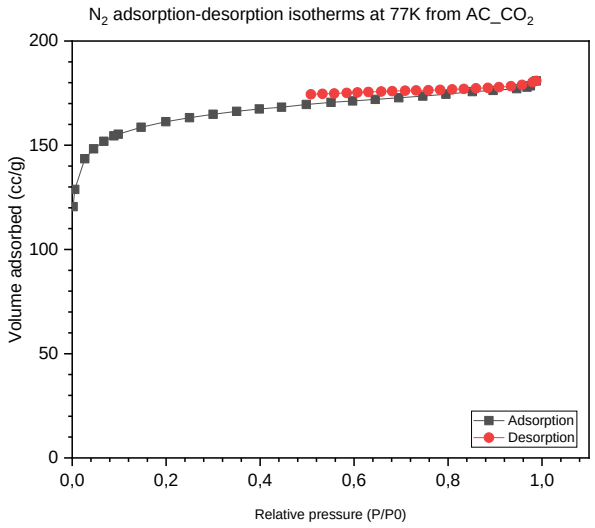

Figure 17 - N_2 adsorpition-desorption isotherms at 77 K from AC_CO_2

A comparable phenomenon was observed in the membranes. A comparison of the membranes with and without the addition of charcoal revealed the presence of pores of varying sizes, indicating the membrane's capacity to form mono and multisolvent membranes. It is notable that the incorporation of activated carbon into the membrane matrix contributed to its development and emphasises its versatility. Figure 18a and 18b illustrate the nitrogen adsorption-desorption isotherms at 77 K for the membranes with formulation 8.

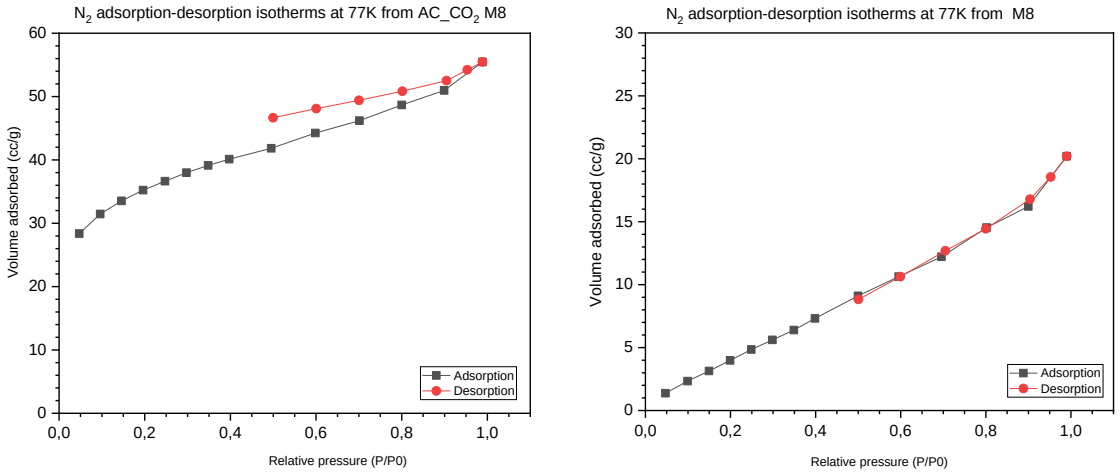

Figure 18 - a) N_2 adsorption-desorpition at 77 K from AC_CO_2 M8; b) from M8

The adsorption isotherm indicates that the incorporation of AC_CO_2 into the membrane, according to Brunauer's classification, resulted in a type II character, indicating the presence

of a system with pores in the range between mesopores and macropores. Upon analysis according to the Giles classification, the isotherms were found to be of the H type for the membrane with AC_CO_2 incorporated. This type of isotherm results in a high affinity between the adsorbate and the adsorbent, with high adsorption and equilibrium being reached. For the membrane that does not contain AC_CO_2 in its matrix, it can be classified in group C, resulting in a linear start, which indicates that the number of active sites is constant in the material. The same pattern is observed for membranes with formulation 14, as illustrated in Figure 19a and 19b.

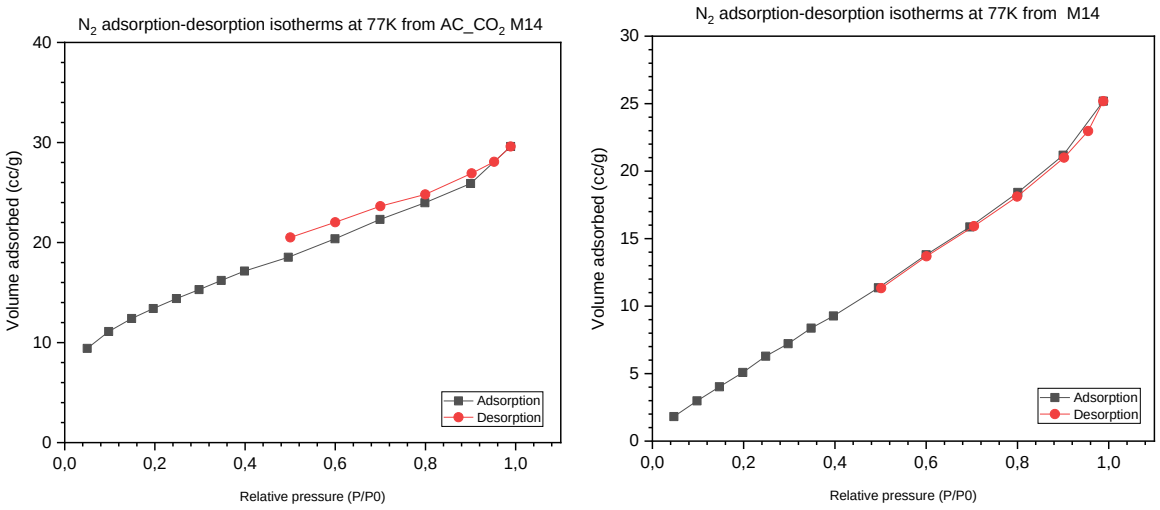

Figure 19 - a) N_2 adsorption-desorpition at 77 K from AC_CO_2 M14; b) from M14

5.3.2 Thermogravimetric Analysis

Thermogravimetric Analysis (TGA) is a widely used primary thermal analysis technique for material characterization. The assay measures the variation in sample mass as a function of the imposed temperature variation on the analyzed material. This technique facilitates the determination of the temperature range at which the material attains a fixed, defined, and constant chemical composition and the temperature at which it begins to decompose, as well as the monitoring of dehydration reactions, oxidation, combustion, decomposition, and other chemical processes that occur as a result of heating. Figure 20 displays the outcomes of the thermogravimetric analyses conducted on EOP and activated carbon. Based on these results, it is possible to conclude about the thermal stability of the samples under analysis.

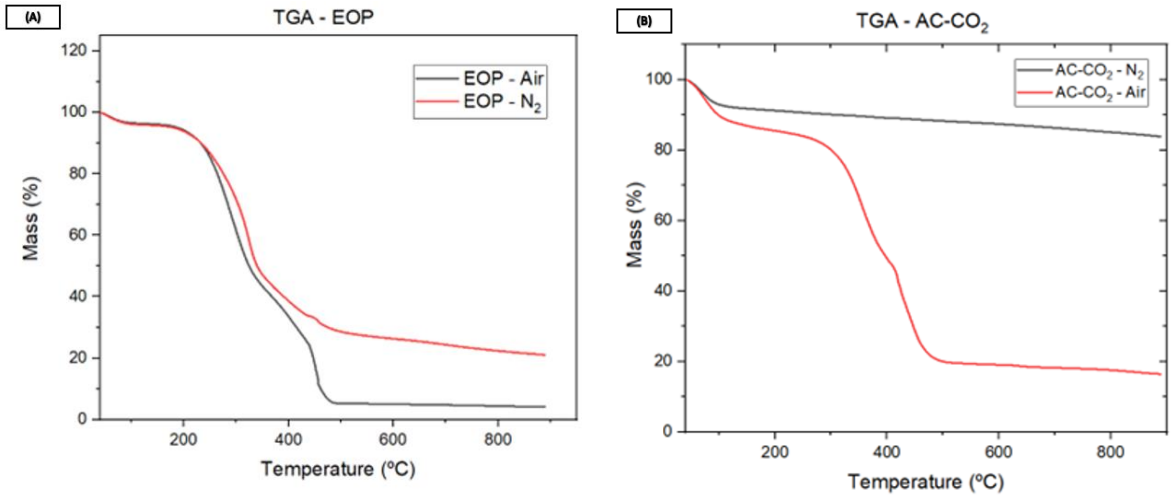

Figure 20 - a) Thermogravimetric analysis of olive pomace; b) Thermogravimetric analysis of activated carbon

Figure 20(a) shows the percentage mass loss for EOP in air and N_2 atmospheres as a function of temperature, while Figure 20(b) shows the same for activated carbon with CO_2 in air and N_2 atmospheres. The text follows conventional academic structure and formatting and follows a logical flow of information with causal links between statements.

The results of the EOP analysis indicate a 95% reduction in mass in an air atmosphere, which is consistent with the percentage of ash analysed in the CNHS characterisation. In a nitrogen atmosphere, an 80% reduction was obtained at the end of the analysis. The analysis revealed three distinct ranges. In the first interval, from 0 to 95°C, the material's moisture is lost in the form of H_2O. In the second interval, from 95 to 182°C, the loss of mass is characterised by the release of volatile components from the decomposition of hemicellulose and cellulose. In the last interval, between 182 and 485°C, the most dense component of the material, lignin, decomposes. This result is consistent with that observed in the study by Bennini et al. (2019)[139] in the same temperature range. The stabilization of the material in both atmospheres commences at 485°C.

The TGA tests, conducted in different atmospheres, demonstrate the differences in the resulting mass of the AC_CO_2 material. The material demonstrated stability at 95°C in an N_2 atmosphere, in accordance with its characteristics following the pyrolysis process, resulting in a final mass loss of approximately 95%. In an air atmosphere, the first moment of mass loss occurs around 110°C, which is associated with the removal of moisture from the sample. The material remains stable between 110°C and 280°C, after which a period of degradation commences until it reaches 500°C. This is related to the release of volatile compounds made up of oxygen and hydrogen, such as the carboxylic compounds left over from the pyrolysis process[140,141]. This corroborates the ash percentages shown in Table 9, which refer to the

elemental analysis of the material.

As illustrated in Figure 21, the AC_CO_2 M8, AC_CO_2 M14, M8 and M14 membranes exhibited comparable behaviour in the thermogravimetric analysis. In both N_2 and air atmospheres, all four membranes exhibited a single stage of thermal degradation.

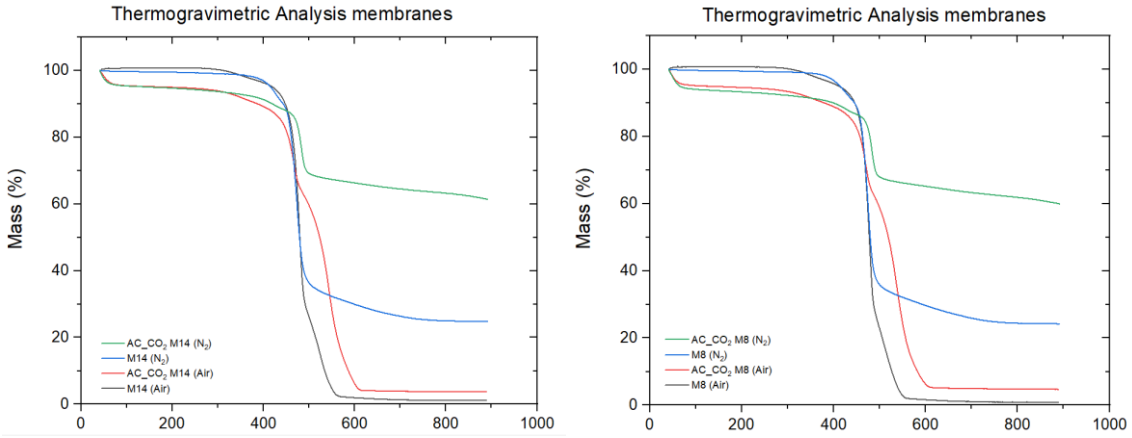

Figure 21 - Thermogravimetric Analysis membranes

As the polymers PVDF and PVP are the basis of their composition, mass loss occurred between 400 and 600°C during the analyses, indicating the specific thermal degradation of each polymer in this range. The PVDF, renowned for its high thermal stability and chemical resistance, is susceptible to significant thermal degradation at elevated temperatures, a process known as defluorination. At this stage, fluorine atoms are lost, resulting in the formation of gases and the decomposition of the polymer, releasing the remaining volatile gases. In contrast, PVP is less thermally stable, with the main polymer chains breaking down in this temperature range, releasing N-vinylpyrrolidone monomers and other smaller fragments. The presence of the pyrrolidone ring in PVP allows for the decomposition of the polymer to result in the release of nitrogen compounds, including ammonia (NH_3), as well as other N_2 derived products. The final mass of the materials in an air atmosphere was less than 5%, indicating that the organic materials present in the membranes had undergone complete thermal degradation.

5.3.3 Fourier-transform infrared spectroscopy

The selection of sample M8 for FTIR analysis was justified by its superior ability to remove the model contaminant compared to other samples evaluated. This selection criterion is essential to ensure that the sample selected is representative of the ideal conditions for the study in question.

Furthermore, the distribution of the bands present in the chemical matrix of sample M8, as shown in Figure 22, is crucial for the analysis of the molecular and functional interactions

involved in the removal of the pollutant. Using FTIR, it is possible to identify the different spectral bands associated with the functional groups present in the sample, allowing a deeper understanding of the adsorption or reaction processes that take place during pollutant removal.

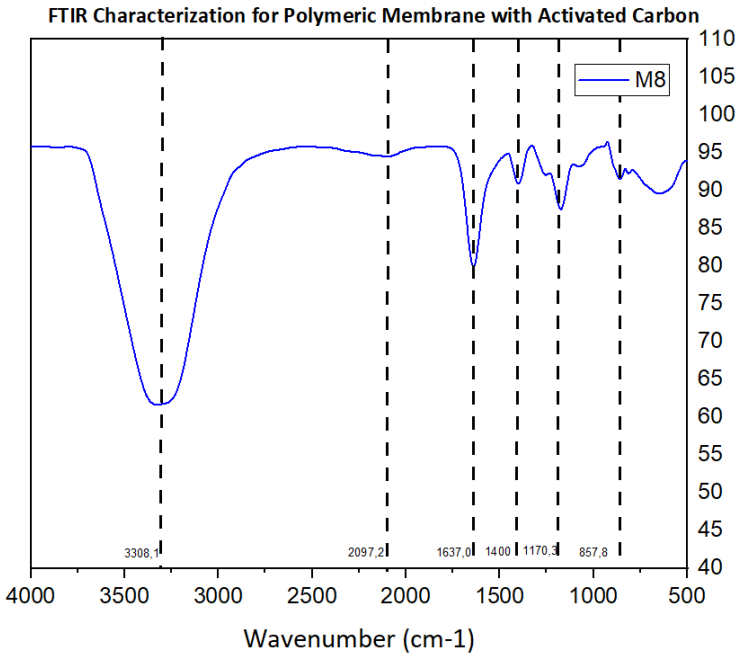

Figure 22 - FTIR Characterization for Polymeric Membrane with Activated Carbon

The spectra show six main peak areas with bands at the values of the OH stretching frequency in the hydroxyl groups (3308 cm^{-1}). The presence of carbonyl groups indicates the presence of oxygen-containing functional groups on the surface of the materials, which act as active sites for adsorption and reaction processes, participating in acid-base reactions and hydrogen bonding. Hydroxyl groups can influence the adsorption behaviour of AC_CO_2 by influencing its interaction with water and other molecules, potentially increasing the affinity of the adsorbent for water and influencing the adsorption of target contaminants. The C - O stretching vibration (1637 cm^{-1}) is known for its chemical stability, which can contribute to the overall stability and durability of the carbonaceous material. The C - H stretching vibration (1400 cm^{-1}) may indicate the presence of aliphatic hydrocarbons or other organic functional groups on the surface of the adsorbents, which may play a role in the adsorption processes by interacting with the adsorbates through van der Waals forces or other interactions. The C-O-C vibrations (1170 cm^{-1}) confirm the presence of aromatic rings in the molecular structure. In the region of 857 cm^{-1}, the observed band is characteristic of the asymmetric stretching of the C-O-C bond present in the secondary ozonide formed by the ozonisation reaction of the coal[148].

5.3.4 Contact angle and pHpzc

The hydrophilicity of the surface of the polymeric membranes and AC_CO_2 was evaluated by measuring the angle of contact with water. According to the data presented in Table 13, it can be observed that all adsorbents had a hydrophilic surface. Dorneles et al. [148] suggest that hydrophilic membranes, which have high chemical resistance, could be considered for use in wastewaters and in the processing of food and pharmaceuticals.

Table 13 - Contact angle and pHpzc

Samples	**pHpzc**	**Contact Angle**	**Hydrophilicity**	**Image**
AC_CO_2 M8	6.58	68±2	Hydrophilic	
AC_CO_2 M14	7.24	56±2	Hydrophilic	
M8	7.62	65±2	Hydrophilic	
M14	7.33	54±2	Hydrophilic	
AC CO_2	10.5	57±2	Hydrophilic	

Figure 23 illustrates the pH_{PCZ} of the materials, including the polymer membranes without the addition of AC_CO_2, membranes with AC_CO_2 and AC_CO_2 itself.

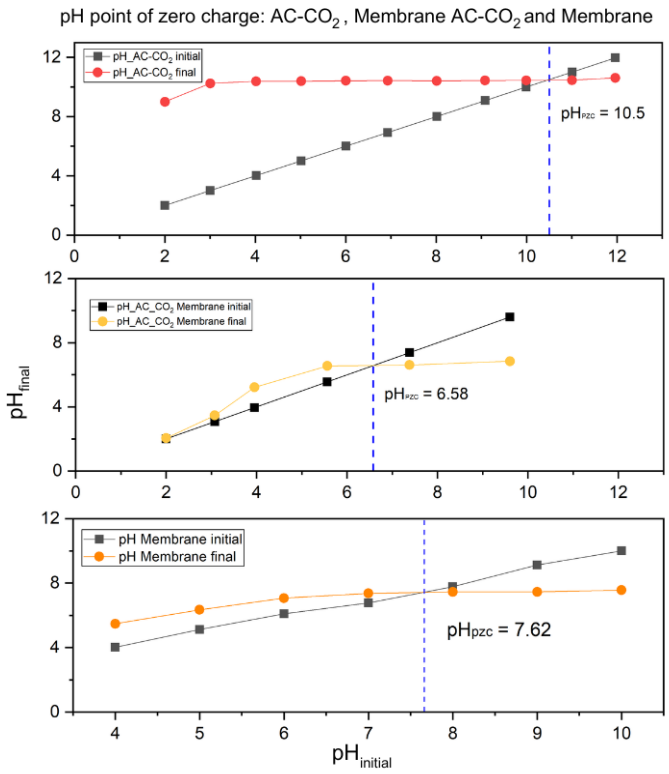

Figure 23 - pH point of zero charge: AC_CO_2, AC_CO_2 M8 and M8.

Upon analysis of the data in conjunction with the values presented in Table 15, which depicts the pH_{PCZ} values for M8 with activated carbon, M8 without activated carbon, and AC-CO_2, respectively, 6.58, 7.62, and 10.5, it becomes evident that the values for the membranes are relatively similar, suggesting the presence of a non-neutralised surface, potentially due to the composition of the polymers present. Conversely, the value for AC-CO_2 is comparable to the pKa of the phenol solution (pKa = 10), resulting in a pH_{PCZ} of 10.5. This indicates that the surface charge of the materials is neutralised, thereby facilitating the adsorption of ions or molecules with opposite charges to the materials. Furthermore, this neutralisation minimises the competition between the ions present in the solution for adsorption on the AC-CO_2 surface. In conclusion, the disparity in pH_{PCZ} values between the membranes and AC-CO_2 exerts a profound influence on the affinity of adsorption and the interaction with chemical species present in the solution.

5.3.5 The surface morphology

The morphology of polymeric membranes M8 and M14, both in their pure form and after the addition of activated carbon, was evaluated by scanning electron microscopy (SEM). Figure 24 shows the SEM images of membrane M8. M8 consists of 1.3 g PVP, 1.15 g PVDF and 8.8 g NMP.

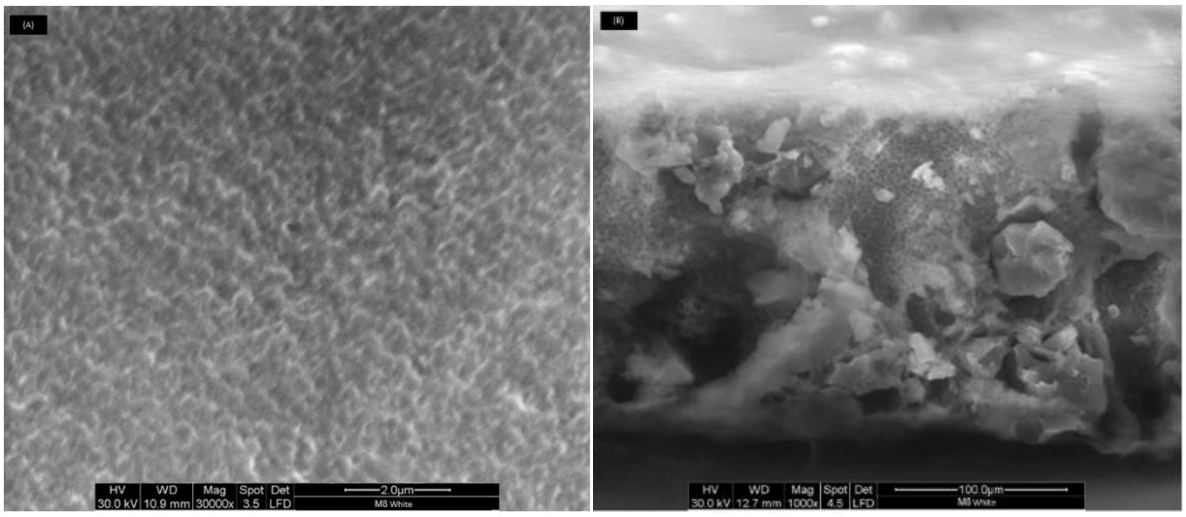

Figure 24 - Scanning Electron Microscopy of Polymeric Membrane 8.

This sample demonstrates a high proportion of PVP and PVDF, resulting in a dense structure and a relatively smooth surface. The manufacturing technique involves casting polymers together with the solvent, resulting in asymmetric structures that promote the separation and selective transport of molecules. Furthermore, it can be observed that the inner part of the membrane contains macropores, which contribute to its mechanical structure and stability. These properties are a result of the hydrophilic and hydrophobic characteristics of the polymers employed. Figure 25 illustrates Polymer membrane 14, which is composed of 0.7g of PVP, 1.15g of PVDF, and 8g of NMP.

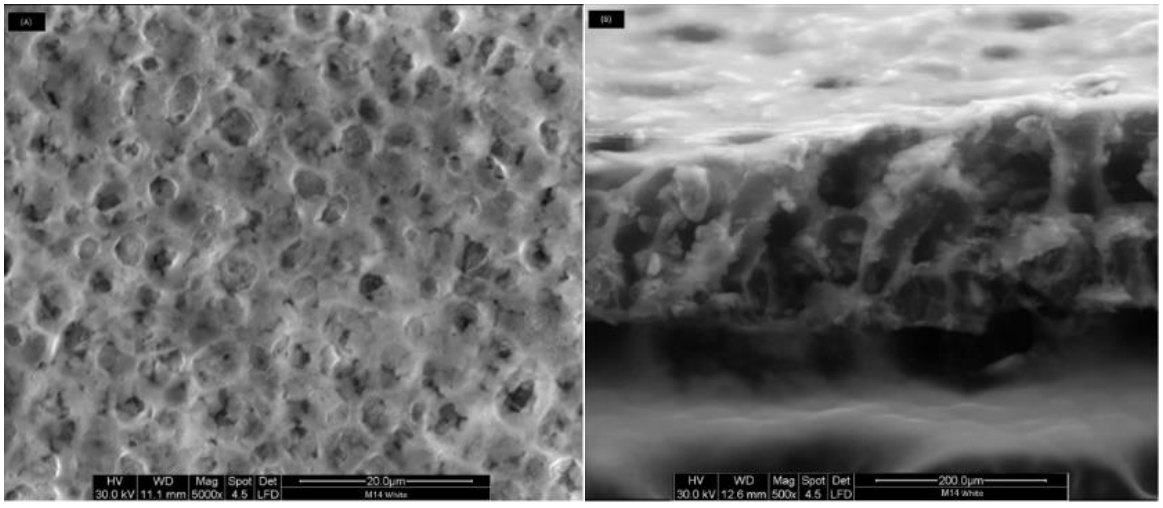

Figure 25 - Scanning Electron Microscopy of Polymeric Membrane 14.

The evidence indicates that the surface of the material is dense and rough, with a greater distribution and size of pores both on and within it. In addition, there are macropores present, which play a pivotal role in the selectivity of the permeating pollutant. The membrane

asymmetric structure, obtained through the phase inversion methodology, results in a significant increase in permeate flux and enhances the membrane transport properties. Figure 26 displays the SEM analysis for the membrane with the same formulation as depicted in Figure 23, but with activated carbon integrated into its polymeric matrix.

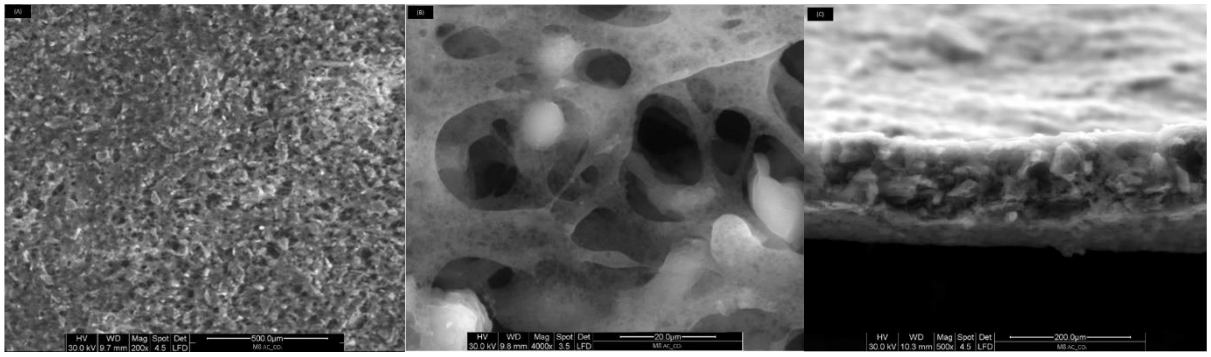

Figure 26 - Scanning electron microscopy was used to examine the polymeric membrane 8 with activated carbon.

The incorporation of AC_CO_2 into the membrane composition has been observed to result in a notable increase in the presence of pores, both on the surface and within. It is important to note that the membrane is asymmetric due to the production process (phase inversion), resulting in a dense surface and a porous internal structure. The incorporation of AC_CO_2 into the polymeric solution confers upon the membrane selective and adsorptive properties, which can enhance adsorption and augment the number of active adsorbent sites. This may facilitate the selection of a broader range of particles and potentially enhance the filtration characteristics. Figure 26c presents a cross-sectional view of the membrane, which comprises two distinct regions: the filtering skin and the support. The filtering skin is responsible for selectivity through the pores, while the support provides the membrane structure and resistance. This characteristic is also observed in the work of Zeni et al[147]. According to their findings, the SEM analysis of the membrane, which has the same composition as the one shown in Figure 25 but includes activated carbon in its polymeric matrix, is displayed in Figure 27.

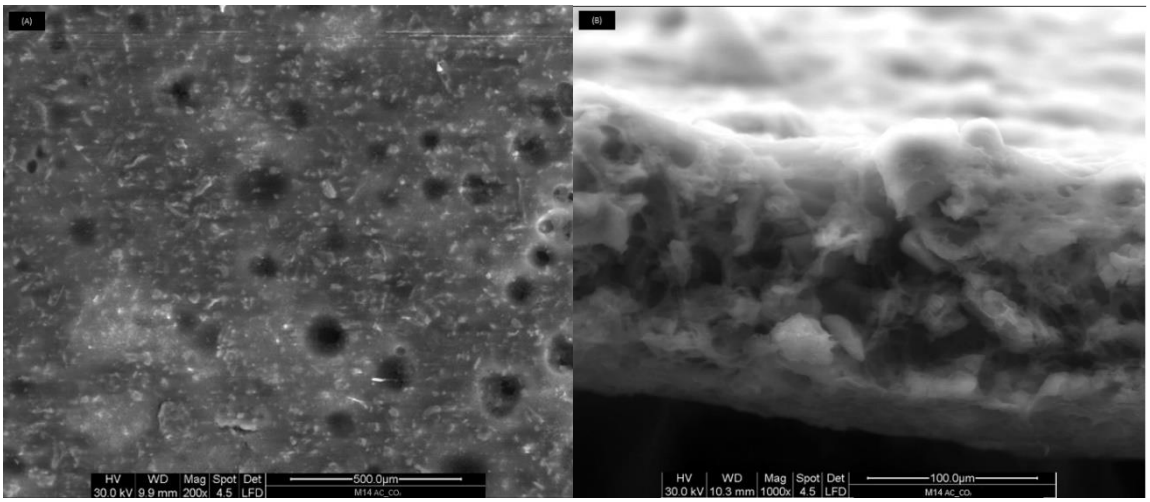

Figure 27 - Scanning Electron Microscopy of Polymeric Membrane 14 with Activated Carbon Incorporation

The outcomes are comparable to those observed in Figure 26, yet the incorporation of activated carbon results in an enhancement of the porosity of the upper layer of the membrane, indicating the presence of larger pores and greater roughness, which are responsible for particle selectivity. Moreover, the interior of the membrane exhibits a more pronounced porous layer, comprising macropores, which contribute to its overall structure and resistance.

5.3.6 Analysis of Polymeric Membranes in a Continuous System

The membrane is distinguished by its high mechanical resistance and hydrophilic nature, which gives it an intrinsic affinity for aqueous solvents. This facilitates the permeation of water and soluble substances[18]. Additionally, the material possesses active sites that are conducive to the filtration and adsorption of these pollutants. These specific characteristics render this material highly effective in addressing the target pollutant, establishing a favourable interaction and optimising the efficiency of the treatment process.

The experiments were conducted on membranes that were sufficiently robust for filtration analysis. A range of thicknesses was selected to enhance the differentiation of adsorption and to evaluate the affinity between the AC_CO_2 and the polymer membranes. During the course of these analyses, a solution containing phenol (50 $mg.L^{-1}$) was employed as a model wastewater in a continuous system, thereby allowing the interaction between the materials to be assessed. The results are presented in Figure 28.

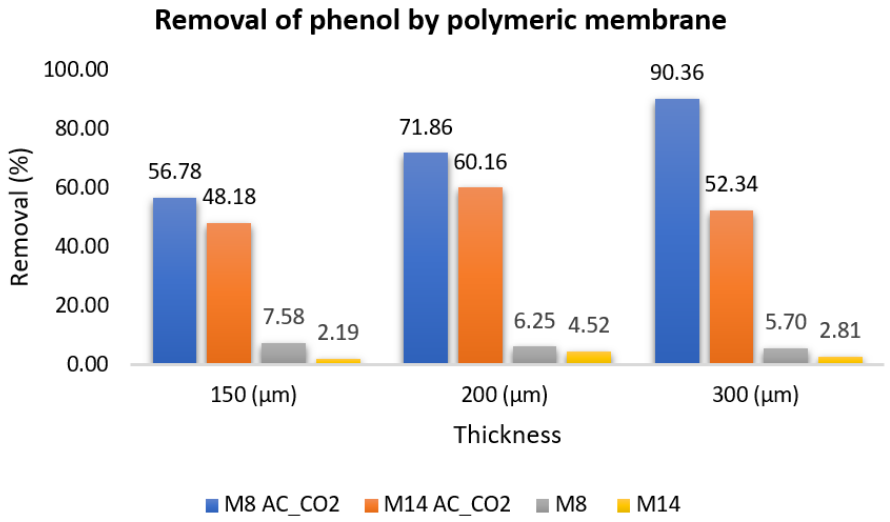

Figure 28 - Removal of phenol by polymeric membrane with AC-CO_2

The results obtained indicate that both membranes with AC-CO_2 in their composition achieved a high level of phenol removal in the first five minutes of analysis. M8 was found to be the most effective in removing phenol in the three different thicknesses tested, with the 300 µm membrane demonstrating the highest performance, achieving 90.36% phenol removal from the model wastewater. Furthermore, M14 demonstrated notable pollutant removal, with a particular achievement of 60.16% removal of the pollutant phenol. Although this removal is lower than that of the M8, it is nevertheless a significant rate and demonstrates the effectiveness of these membranes in removing phenol. The membranes lacking the presence of AC_CO_2 exhibited a comparatively lower performance, with a low removal rate observed across the three distinct thicknesses. This outcome serves to highlight the significant efficacy of AC_CO_2 addition, which has been demonstrated to enhance pollutant removal through the increased distribution of active sites on the membrane surface.

6. CONCLUSIONS

This study aimed to investigate the production and characterisation of activated carbon derived from olive pomace (EOP) and its incorporation into polymeric membranes. The utilisation of EOP as a precursor for the production of activated carbon (AC_CO_2) was advantageous due to its accessibility, abundance, and potential for waste valorisation in the region. The carbonisation process resulted in a notable alteration of the material's chemical composition, with an increase in carbon content from 49.1% in EOP to 62.65% in AC_CO_2. The resulting activated carbon exhibited enhanced adsorption properties, which were confirmed through kinetic and equilibrium adsorption studies for phenol removal. The pseudo-second-order kinetic model provided the most accurate fit for the adsorption data, indicating the formation of valence forces between the adsorbent and adsorbate.

Furthermore, equilibrium isotherm analysis indicated that the Freundlich model, which describes adsorption on heterogeneous surfaces, was the most suitable fit for the data, thereby highlighting the material's high adsorption capacity. The polymeric membranes prepared, in particular the formulations M8 and M14, exhibited promising mechanical strength, adsorption capacity, and porosity, rendering them suitable for separation and purification applications.

The utilisation of characterisation techniques, including BET surface area analysis, TGA, FTIR, contact angle measurements, and SEM, enabled the comprehensive elucidation of the physical and chemical properties of the materials.

The BET analysis revealed a significant degree of porosity in AC_CO_2, which is essential for effective adsorption processes. TGA demonstrated the thermal stability of the materials, while FTIR identified the functional groups that are crucial for adsorption. Contact angle measurements indicated that the membranes exhibited hydrophilic properties, thereby enhancing their applicability in aqueous environments.

The SEM analysis revealed the morphological characteristics of the membranes, demonstrating a dense surface with varying pore sizes and a porous internal structure. These characteristics are vital for effective filtration and pollutant removal. The incorporation of AC_CO_2 into the membranes enhanced their structural integrity and increased the number of active adsorption sites.

Overall, this study successfully demonstrated the potential of utilising olive pomace-derived activated carbon in the development of advanced polymeric membranes for environmental applications. The findings contribute to the sustainable management of agricultural waste and the advancement of materials for water treatment and pollutant removal. Future research should focus on optimising the production processes and exploring the long-term performance and

regeneration of these membranes in real-world applications.

7. FUTURE WORKS SUGGESTIONS

Suggestions for future work

- Develop effective methods to regenerate the activated carbon used in the membranes, thereby increasing their useful life and sustainability.
- Long-term studies are required to determine the stability and effectiveness of the membranes under real operating conditions.
- The efficacy of the membranes in the removal of pollutants from a range of industrial and municipal wastewater sources will be evaluated.
- The ability of membranes to remove a variety of contaminants, including heavy metals, organic compounds and microplastics, is to be evaluated.
- The development and testing of laboratory-scale wastewater treatment systems using membranes with activated carbon is to be undertaken with a view to validating their practical effectiveness.

8. REFERENCES

1. Carvalho, F. T. A agenda 2030 para o desenvolvimento sustentável da onu e seus atores: o impacto do desenvolvimento sustentável nas relações internacionais. Open journal systems 13, 104–116 (2019).
2. Reis, M. P., Ferreira, R. M. de O. Q. & Ferreira, L. M. G. de A. Estudo de processos de tratamento de águas residuais de lagares de azeite. (2016).
3. Vieira, D. C. S. M., Gonçalves, A. & Feliciano Jesus Joaquim, M. Análise do Ciclo de Vida do Azeite: Caso de estudo do azeite de Trás-os-Montes. (2014).
4. Duman, A. K., Özgen, G. Ö. & Üçtuğ, F. G. Environmental life cycle assessment of olive pomace utilization in Turkey. Sustain Prod Consum 22, 126–137 (2020).
5. Soares, B. M. Pré-tratamentos aquosos do bagaço e caroço de azeitona para obtenção de compostos de valor acrescentado. Lisboa: ISA, 59, (2019).
6. Fernández-Lobato, L. et al. Life cycle assessment of the Spanish virgin olive oil production: A case study for Andalusian region. J Clean Prod 290, (2021).
7. Elkacmi, R. & Bennajah, M. Advanced oxidation technologies for the treatment and detoxification of olive mill wastewater: A general review. Journal of Water Reuse and Desalination 9, 463–505 (2019).
8. Almeida, M. S. D. Tratamento e valorização de efluentes de lagares de azeite integrando processos de membranas, adsorção/permute iónica e oxidação avançada (Master's thesis), (2016).
9. Arbizu-Milagro, J., Castillo-Ruiz, F. J., Tascón, A. & Peña, J. M. How Could Precision Irrigation Based on Daily Trunk Growth Improve Super High-Density Olive Orchard Irrigation Efficiency Agronomy 12, (2022).
10. Hannachi, H. et al. Fatty acids, sterols, polyphenols, and chlorophylls of olive oils obtained from tunisian wild olive trees (olea europaea l. var. sylvestris). Int J Food Prop 16, 1271–1283 (2013).
11. Mieziene, B. et al. Adherence to Mediterranean diet among Lithuanian and Croatian students during COVID-19 pandemic and its health behavior correlates. Front Public Health 10, (2022).
12. Marrone, G. et al. Extra Virgin Olive Oil and Cardiovascular Protection in Chronic Kidney Disease. Nutrients 14, (2022).
13. Ponnampalam, E. N. et al. The Importance of Dietary Antioxidants on Oxidative Stress, Meat and Milk Production, and Their Preservative Aspects in Farm Animals: Antioxidant Action, Animal Health, and Product Quality—Invited Review. Animals vol. 12 Preprint at https://doi.org/10.3390/ani12233279 (2022).
14. Carrión, Y., Ntinou, M. & Badal, E. Olea europaea L. in the North Mediterranean Basin during the Pleniglacial and the Early–Middle Holocene. Quat Sci Rev 29, 952–968 (2010).
15. Platis, D. P., Menexes, G. C., Kalburtji, K. L. & Mamolos, A. P. Energy budget, carbon and water footprint in perennial agro and natural ecosystems inside a Natura 2000 site as provisioning and regulating ecosystem services. Environmental Science and Pollution Research 30, 1288–1305 (2023).
16. Conselho Oleícola Internacional (2020). COI-Unidade de Assuntos Económicos e

Promoção.www.internationaloliveoil.org/what-we-do/economic-affairs-promotion-unit/#figures (2020).
17. Sales, H., Figueiredo, F., Vaz Patto, M. C. & Nunes, J. Assessing the environmental sustainability of Portuguese olive growing practices from a life cycle assessment perspective. J Clean Prod 355, 131692 (2022).
18. Friedeberg, A. S. Olive oil in the EC. Food Policy 8, 13–22 (2020).
19. Muniz, F. G. Mapeamento de resíduos e subprodutos derivados da extração de azeites da região do alentejo. (Master's thesis) (2021).
20. Yanık, D. K. Alternative to traditional olive pomace oil extraction systems: Microwave-assisted solvent extraction of oil from wet olive pomace. LWT 77, 45–51 (2017).
21. Domingues, E., Fernandes, E., Gomes, J., Castro-Silva, S. & Martins, R. C. Olive oil extraction industry wastewater treatment by coagulation and Fenton's process. Journal of Water Process Engineering 39, 101818 (2021).
22. Salgueiro, C., Anjos, O. & Peres, F. Projeto Promoção e Valorização de Azeites de Montanha. 25–36 (2019).
23. Restuccia, D., Prencipe, S. A., Ruggeri, M. & Spizzirri, U. G. Sustainability Assessment of Different Extra Virgin Olive Oil Extraction Methods through a Life Cycle Thinking Approach: Challenges and Opportunities in the Elaio-Technical Sector. Sustainability (Switzerland) 14, (2022).
24. Fernández-Lobato, L. et al. Life cycle assessment of the Spanish virgin olive oil production: A case study for Andalusian region. J Clean Prod 290, 125677 (2021).
25. Manuel, A., Caetano, V., Doutora, O. :, Maria, E. & Ramalho, R. Valorização do Bagaço de Azeitona: Dimensionamento de um Extrator Sólido-Líquido. (2020).
26. Esquivel, M. M. et al. Supercritical Carbon Dioxide Extraction of SardineSardina pilchardusOil. LWT - Food Science and Technology 30, 715–720 (1997).
27. Mukhopadhyay, M. Extratos Naturais Usando Dióxido de Carbono Supercrítico. 2000 (2000). doi:https://doi.org/10.1201/9781420041699.
28. Tomás, M. B. B. Optimization of laboratory control processes and analysis of factors that influence the extraction and quality of olive pomace oil. MSc thesis, Faculdade de Ciências e Tecnologia da Universidade Nova de Lisboa: Lisbon, Portugal, 2018, 138p 138 (2018).
29. Freitas, M. R. De. Avaliação Do Potencial Energético Dos Resíduos Sólidos Dos Lagares Do Alentejo. p 0–180, (2007).
30. Sansoucy, R. Utilisation des sous-produits de l'olivier en alimentation animale dans le bassin Méditerranéen. Preprint at (1984).
31. Silva, F. D., Alves Queiroz Da Silva, A. M., Ribeiro, A. M. E. & Brito, P. M. P. Processos termoquímicos de conversão de biomassa. (2021).
32. Limayem, A. & Ricke, S. C. Lignocellulosic biomass for bioethanol production: Current perspectives, potential issues and future prospects. Prog Energy Combust Sci 38, 449–467 (2012).
33. Srivastava, A., Mathur, P. K. & Sharma, V. P. Studies of wastewater treatment techniques using low-cost biosorbents. in Microbial Ecology of Wastewater Treatment Plants (eds. Shah, M. & Rodriguez-Couto, S.) 395–410 (Elsevier, 2021). doi:https://doi.org/10.1016/B978-0-12-822503-5.00001-1.

34. Monte, H. M. Tratamento de águas residuais de tratamento biológico. (2018).
35. Zahi, M. R., Zam, W. & El Hattab, M. State of knowledge on chemical, biological and nutritional properties of olive mill wastewater. Food Chem 381, 132238 (2022).
36. Davies, L. C., Vilhena, A. M., Novais, J. M. & Martins-Dias, S. Olive mill wastewater characteristics: Modelling and statistical analysis. Grasas y Aceites 55, 233–241 (2004).
37. Oreopoulou, Vasso. & Russ, Winfried. Utilization of By-Products and Treatment of Waste in the Food Industry. (Springer, 2007).
38. Esteves, B. M., Rodrigues, C. S. D., Maldonado-Hódar, F. J. & Madeira, L. M. Treatment of high-strength olive mill wastewater by combined Fenton-like oxidation and coagulation/flocculation. J Environ Chem Eng 7, (2019).
39. Kipper, M. Universidade federal do rio grande do sul Biorreatores com Membranas : uma Alternativa para o Tratamento de Efluentes Biorreatores com Membranas : uma Alternativa para o Tratamento de Efluentes. (2009).
40. Decreto-Lei n.º 236/98, de 1 de Agosto.
41. Recolha, R. G. De. Regulamento Geral De Recolha, Tratamento E Rejeição De Efluentes Do Sistema De Santo André (Rgesa). 1–30.
42. Víctor-Ortega, M. D., Ochando-Pulido, J. M. & Martínez-Ferez, A. Performance and modeling of continuous ion exchange processes for phenols recovery from olive mill wastewater. Process Safety and Environmental Protection 100, 242–251 (2016).
43. Cruz, A. P. G. Recuperação de compostos bioativos a partir de resíduos da indústria vitivinícola. Rev Bras Frutic 35, 1147–1157 (2013).
44. Tekin, A. R. & Dalgıç, A. C. Biogas production from olive pomace. Resour Conserv Recycl 30, 301–313 (2000).
45. Gómez-Casero, M. A., Moral-Moral, F. J., Pérez-Villarejo, L., Sánchez-Soto, P. J. & Eliche-Quesada, D. Synthesis of clay geopolymers using olive pomace fly ash as an alternative activator. Influence of the additional commercial alkaline activator used. Journal of Materials Research and Technology 12, 1762–1776 (2021).
46. Zhang, K., Zhao, H. & Wang, S. C. Upcycle olive pomace as antioxidant and recycling agent in asphalt paving materials. Constr Build Mater 330, 127217 (2022).
47. Aguado, R., Vera, D., Jurado, F. & Beltrán, G. An integrated gasification plant for electric power generation from wet biomass: toward a sustainable production in the olive oil industry. Biomass Convers Biorefin (2022) doi:10.1007/s13399-021-02231-0.
48. Alcazar-Ruiz, A., Dorado, F. & Sanchez-Silva, L. Bio-phenolic compounds production through fast pyrolysis: Demineralizing olive pomace pretreatments. Food and Bioproducts Processing 137, 200–213 (2023).
49. Alcazar-Ruiz, A., Garcia-Carpintero, R., Dorado, F. & Sanchez- Silva, L. Valorization of olive oil industry subproducts: ash and olive pomace fast pyrolysis. Food and Bioproducts Processing 125, 37–45 (2021).
50. Ouazzani, W. T., Farissi, L. E., Monteiro, E. & Rouboa, A. Automotive plastic waste and olive pomace valorization using the pyrolysis process. Energy Reports 8, 628–637 (2022).
51. Fokaides, P. A. Energy recovery alternatives of the olive oil industry byproducts. in European Biomass Conference and Exhibition Proceedings vol. 2018 83–87 (2018).
52. Gomez-Martin, A., Chacartegui, R., Ramirez-Rico, J. & Martinez-Fernandez, J.

Performance improvement in olive stone's combustion from a previous carbonization transformation. Fuel 228, 254–262 (2018).
53. Ochando-Pulido, J. M., Vellido-Pérez, J. A., González-Hernández, R. & Martínez-Férez, A. Optimization and modeling of two-phase olive-oil washing wastewater integral treatment and phenolic compounds recovery by novel weak-base ion exchange resins. Sep Purif Technol 249, 117084 (2020).
54. Windeatt, J. H. et al. Characteristics of biochars from crop residues: Potential for carbon sequestration and soil amendment. J Environ Manage 146, 189–197 (2014).
55. Hassanein, M. M., Al-Amrossy, E. F., Abo-Elwafa, G. A. & Abdel-Razek, A. G. Characterization of Egyptian Monovarietal Koroneiki Virgin Olive Oil and Its Co-Products. Egypt J Chem 65, 637–645 (2022).
56. Mullen, C. A. et al. Bio-oil and bio-char production from corn cobs and stover by fast pyrolysis. Biomass Bioenergy 34, 67–74 (2010).
57. Zhang, M. et al. Pyrolysis of Ca/Fe-rich antibiotic fermentation residues into biochars for efficient phosphate removal/recovery from wastewater: Turning hazardous waste to phosphorous fertilizer. Science of the Total Environment 869, (2023).
58. DING, Y. et al. Potential Benefits of Biochar in Agricultural Soils: A Review. Pedosphere 27, 645–661 (2017).
59. James, A., Sánchez, A., Prens, J. & Yuan, W. Biochar from agricultural residues for soil conditioning: Technological status and life cycle assessment. Curr Opin Environ Sci Health 25, 100314 (2022).
60. Dilokekunakul, W., Teerachawanwong, P., Klomkliang, N., Supasitmongkol, S. & Chaemchuen, S. Effects of nitrogen and oxygen functional groups and pore width of activated carbon on carbon dioxide capture: Temperature dependence. Chemical Engineering Journal 389, (2020).
61. Cho, S.-H. et al. Applications of agricultural residue biochars to removal of toxic gases emitted from chemical plants: A review. Science of the Total Environment 868, (2023).
62. Shaikhiev, I. G., Kraysman, N. V. & Sverguzova, S. V. Review of Peach (Prúnus pérsica) Shell Use to Remove Pollutants from Aquatic Environments. Biointerface Res Appl Chem 13, (2023).
63. Wagner, N. J. & Jula, R. J. Activated Carbon Adsorption. Activated Carbon Adsorption For Wastewater Treatment (2018). doi:10.1201/9781351069465-3.
64. Alicia Peláez-Cid, A. & Teutli-León, M. M. M. Lignocellulosic Precursors Used in the Elaboration of Activated Carbon. (2012).
65. da Silva Lima, P. N. et al. Advanced sustainable carbon material from babassu biomass and its adsorption performance. Journal of Physics and Chemistry of Solids 176, (2023).
66. Shaikhiev, I. G., Kraysman, N. V. & Sverguzova, S. V. Review of Peach (Prúnus pérsica) Shell Use to Remove Pollutants from Aquatic Environments. Biointerface Res Appl Chem 13, (2023).
67. Guimarães, T., De Oliveira, A. F., Lopes, R. P. & De Carvalho Teixeira, A. P. Biochars obtained from arabica coffee husks by a pyrolysis process: Characterization and application in Fe(ii) removal in aqueous systems. New Journal of Chemistry 44, 3310–3322 (2020).
68. Mona, S. et al. Towards sustainable agriculture with carbon sequestration, and

greenhouse gas mitigation using algal biochar. Chemosphere 275, (2021).
69. El Hassani, F. Z., Errachidi, F., Aissam, H., Merzouki, M. & Benlemlih, M. Effect of Olive Mill Wastewater on the composition of the essential oil of bergamot-mint under semi-arid climate. Ind Crops Prod 177, 114487 (2022).
70. Sparrevik, M., Field, J. L., Martinsen, V., Breedveld, G. D. & Cornelissen, G. Life cycle assessment to evaluate the environmental impact of biochar implementation in conservation agriculture in Zambia. Environ Sci Technol 47, 1206–1215 (2013).
71. Crini, G. & Lichtfouse, E. Advantages and disadvantages of techniques used for wastewater treatment. Environ Chem Lett 17, 145–155 (2019).
72. Ng, C., Losso, J. N., Marshall, W. E. & Rao, R. M. Physical and chemical properties of selected agricultural byproduct-based activated carbons and their ability to adsorb geosmin. Bioresour Technol 84, 177–185 (2002).
73. Ng, C., Losso, J. N., Marshall, W. E. & Rao, R. M. Freundlich adsorption isotherms of agricultural by-product-based powdered activated carbons in a geosmin-water system. Bioresour Technol 85, 131–135 (2002).
74. Nobre, J. R. C. et al. Characterization of activated carbon produced from sawdust massaranduba. Scientia Forestalis/Forest Sciences 43, 693–702 (2015).
75. Gorgulho, H. F., Mesquita, J. P., Gonçalves, F., Pereira, M. F. R. & Figueiredo, J. L. Characterization of the surface chemistry of carbon materials by potentiometric titrations and temperature-programmed desorption. Carbon N Y 46, 1544–1555 (2008).
76. Suzuki, R. M., Andrade, A. D., Sousa, J. C. & Rollemberg, M. C. Preparation and characterization of activated carbon from rice bran. Bioresour Technol 98, 1985–1991 (2007).
77. Heylmann, K. K. A. et al. Production, characterization, and application of activated charcoal from peach kernel in textile effluent treatment. Engenharia Sanitaria e Ambiental 26, 485–494 (2021).
78. IUPAC. International Union of Pure and Applied Chemistry. Physical Chemistry ii https://iupac.org/ (2023) doi:10.1016/b978-0-08-022036-9.50001-9.
79. Ferraz, M. M. P. de F. Contribuição para o estudo do tratamento de efluentes de lagares de azeite. (2012).
80. Panizio, R. M. Tratamento e valorização energética de efluentes da indústria corticeira. (2020).
81. Melin, T. et al. Membrane bioreactor technology for wastewater treatment and reuse. Desalination 187, 271–282 (2006).
82. Zscherpe, C., Weissgerber, C. & Schwermann, S. Development of a reverse osmosis and nanofiltration membrane cascade to produce skim milk concentrate. J Food Eng 343, (2023).
83. Song, J. et al. Unsaturated single-atom CoN<inf>3</inf> sites for improved fenton-like reaction towards high-valent metal species. Appl Catal B 325, (2023).
84. Proietti, S. et al. Extra Virgin Olive oil as carbon negative product: Experimental analysis and validation of results. J Clean Prod 166, 550–562 (2017).
85. Tan, S. et al. Utilization of current pyrolysis technology to convert biomass and manure waste into biochar for soil remediation: A review. Science of The Total Environment 864, 160990 (2023).

86. Fu, J., Yan, B., Gui, S., Fu, Y. & Xia, S. Anaerobic co-digestion of thermo-alkaline pretreated microalgae and sewage sludge: Methane potential and microbial community. J Environ Sci (China) 127, 133–142 (2023).
87. Wang, R. et al. Chemical modification of straw hydrochar as additive to improve the anaerobic digestion performance of sludge hydrothermal carbonization wastewater. Fuel 340, (2023).
88. Mishra, S. et al. Anaerobic–aerobic treatment of wastewater and leachate: A review of process integration, system design, performance and associated energy revenue. J Environ Manage 327, (2023).
89. Garcés, L. F. & Penuela, G. A. Fotocatálisis de las aguas residuales de la industria textil utilizando colector solar. Rev. Lasallista Investig 4, 24–31 (2012).
90. Araujo, K. S., Antonelli, R. & Gaydesczka, B. Processos oxidativos avançados: uma revisão de fundamentos e aplicações no tratamento de águas residuais urbanas e efluentes industriais. Revista Ambiente e Agua 9, 445–458 (2016).
91. Chan, Y. J., Chong, M. F., Law, C. L. & Hassell, D. G. A review on anaerobic–aerobic treatment of industrial and municipal wastewater. Chemical Engineering Journal 155, 1–18 (2009).
92. Vuppala, S. et al. Multistage treatment for olive mill wastewater: Assessing legal compliance and operational costs. J Environ Chem Eng 10, 107442 (2022).
93. Cadore, Í. R. Efeito das condições hidrodinâmicas no desempenho de um Biorreator com Membranas Submersas em pressão constante. (2015).
94. Jang, D., Lee, J. & Jang, A. Impact of pre-coagulation on the ceramic membrane process during oil-water emulsion separation: Fouling behavior and mechanism. Chemosphere 313, 137596 (2023).
95. Guo, W., Ngo, H.-H. & Li, J. A mini-review on membrane fouling. Bioresour Technol 122, 27–34 (2012).
96. Poletto, P. et al. Avaliação das características de transporte em membranas de poliamida 66 preparadas com diferentes solventes. Polimeros 22, 273–277 (2012).
97. Thürmer, M. B., Poletto, P., Marcolin, M., Ferreira, D. G. & Andrade, M. Z. Preparação e caracterização de membranas assimétricas de poli(fluoreto de vinilideno) suportadas em poliéster-i.
98. Sukitpaneenit, P. & Chung, T.-S. Molecular design of the morphology and pore size of PVDF hollow fiber membranes for ethanol–water separation employing the modified pore-flow concept. J Memb Sci 374, 67–82 (2011).
99. Liu, F., Hashim, N. A., Liu, Y., Abed, M. R. M. & Li, K. Progress in the production and modification of PVDF membranes. J Memb Sci 375, 1–27 (2011).
100. Pereira, A. Os Processos De Separação Por Membranas No Tratamento De Água Para Abastecimento : Revisão Bibliográfica. 1–17 (2018).
101. Zhang, H., Du, L., Xing, J., Wei, G. & Quan, X. Electro-conductive crosslinked polyaniline/carbon nanotube nanofiltration membrane for electro-enhanced removal of bisphenol A. Front Environ Sci Eng 17, (2023).
102. Meyer, P., Hartinger, M., Sigler, S. & Kulozik, U. Concentration of Milk and Whey by Membrane Technologies in Alternative Cascade Modes. Food Bioproc Tech 10, 674–686 (2017).

103. Januário, E. F. D., Vidovix, T. B., Bergamasco, R. & Vieira, A. M. S. Performance of a hybrid coagulation/flocculation process followed by modified microfiltration membranes for the removal of solophenyl blue dye. Chemical Engineering and Processing - Process Intensification 168, (2021).
104. Bhattacharya, P., Mukherjee, D., Deb, N., Swarnakar, S. & Banerjee, S. Application of green synthesized ZnO nanoparticle coated ceramic ultrafiltration membrane for remediation of pharmaceutical components from synthetic water: Reusability assay of treated water on seed germination. J Environ Chem Eng 8, (2020).
105. Pérez Donato, J. A., Vera, L., Bravo, S. L., Delgado, S. & González, E. Effects of ultrafiltration on the phytotoxicity of primary and secondary effluents from urban wastewater treatment | Efectos de la ultrafiltración sobre la fitotoxicidad de efluentes primarios y secundarios de la depuración de aguas residuales urbanas. Revista de Toxicologia 33, 103–107 (2016).
106. Khan, A. A. & Boddu, S. Hybrid Membrane Process: An Emerging and Promising Technique toward Industrial Wastewater Treatment. Membrane-based Hybrid Processes for Wastewater Treatment (2021). doi:10.1016/B978-0-12-823804-2.00002-1.
107. Sinha, N. & Dahiya, P. Chapter 10 - Removal of emerging contaminants from pharmaceutical wastewater through application of bionanotechnology. in (eds. Shah, M., Rodriguez-Couto, S. & Biswas, J. B. T.-D. in W. T. R. and P.) 247–264 (Elsevier, 2022). doi:https://doi.org/10.1016/B978-0-323-85583-9.00004-1.
108. Roy, S. et al. Removal of heavy metals by surface tailored copper ion enhanced ceramic-supported-polymeric composite nanofiltration membrane. J Environ Chem Eng 9, (2021).
109. Zhang, R. et al. Antifouling membranes for sustainable water purification: Strategies and mechanisms. Chem Soc Rev 45, 5888–5924 (2016).
110. Malliga, P., Bela, R. B. & Shanmugapriya, N. Chapter 5 - Conversion of textile effluent wastewater into fertilizer using marine cyanobacteria along with different agricultural waste. in (eds. Krishnaraj Rathinam, N. & Sani, R. K. B. T.-B. of W. to R. C. and B.) 87–111 (Elsevier, 2020). doi:https://doi.org/10.1016/B978-0-12-817951-2.00005-5.
111. Wai, K. P., Koo, C. H., Pang, Y. L., Chong, W. C. & Lau, W. J. Purifying surface waters contaminated with natural organic matters and bacteria using Ag/PDA-coated PES membranes. Environmental Engineering Research 28, (2023).
112. Radmanesh, F., Bargeman, G. & Benes, N. E. Cyclomatrix polyphosphazene organic solvent nanofiltration membranes. J Memb Sci 668, (2023).
113. Tahmasebi, E. & Mirzania, R. Polyaniline-polycaprolactone electrospun nanofibrous mat: new polymeric support with anion exchange characteristic for immobilizing liquid membrane in efficient on-chip electromembrane extraction of polar acidic drugs. Microchimica Acta 190, (2023).
114. Wu, L., Sun, J. & Wang, Q. Poly(vinylidene fluoride)/polyethersulfone blend membranes: Effects of solvent sort, polyethersulfone and polyvinylpyrrolidone concentration on their properties and morphology. J Memb Sci 285, 290–298 (2006).
115. Kachhadiya, D. D. & Murthy, Z. V. P. Microfluidic synthesized ZIF-67 decorated PVDF mixed matrix membranes for the pervaporation of toluene/water mixtures. J

Memb Sci 676, (2023).
116. Yasir, A. T., Benamor, A., Hawari, A. H. & Mahmoudi, E. Poly (amido amine) dendrimer based membranes for wastewater treatment – A critical review. Chem Eng Sci 273, (2023).
117. Morais, D. C. et al. Combining Polymer and Cyclodextrin Strategy for Drug Release of Sulfadiazine from Electrospun Fibers. Pharmaceutics 15, (2023).
118. Kartohardjono, S., Salsabila, G. M. K., Ramadhani, A., Purnawan, I. & Lau, W. J. Preparation of PVDF-PVP Composite Membranes for Oily Wastewater Treatment. Membranes (Basel) 13, (2023).
119. Nayab, S. S. et al. Anti-foulant ultrafiltration polymer composite membranes incorporated with composite activated carbon/chitosan and activated carbon/thiolated chitosan with enhanced hydrophilicity. Membranes (Basel) 11, (2021).
120. Karki, S. & Ingole, P. G. Development of polymer-based new high performance thin-film nanocomposite nanofiltration membranes by vapor phase interfacial polymerization for the removal of heavy metal ions. Chemical Engineering Journal 446, 137303 (2022).
121. Arandia, K., Karna, N. K., Mattsson, T., Larsson, A. & Theliander, H. Fouling characteristics of microcrystalline cellulose during cross-flow microfiltration: Insights from fluid dynamic gauging and molecular dynamics simulations. J Memb Sci 669, 121272 (2023).
122. Ribeiro, R. S. et al. Synthesis of low-density polyethylene derived carbon nanotubes for activation of persulfate and degradation of water organic micropollutants in continuous mode. J Environ Manage 308, (2022).
123. Al-Maliky, E. A., Gzar, H. A. & Al-Azawy, M. G. Determination of Point of Zero Charge (PZC) of Concrete Particles Adsorbents. IOP Conf Ser Mater Sci Eng 1184, 012004 (2021).
124. Al-Ghouti, M. A. & Al-Absi, R. S. Mechanistic understanding of the adsorption and thermodynamic aspects of cationic methylene blue dye onto cellulosic olive stones biomass from wastewater. Sci Rep 10, 1–18 (2020).
125. Campos, S. Análise De Isotermas De Adsorção Da Cafeína Em Diferentes Adsorventes E Dimensionamento De Um Pré-Projeto De Uma Unidade De Adsorção. (2020).
126. Eshghabadi, F. & Javanbakht, V. Preparation of porous metakaolin-based geopolymer foam as an efficient adsorbent for dye removal from aqueous solution. J Mol Struct 1295, (2024).
127. Mirizadeh, S., Solisio, C., Converti, A. & Casazza, A. A. Efficient removal of tetracycline, ciprofloxacin, and amoxicillin by novel magnetic chitosan/microalgae biocomposites. Sep Purif Technol 329, (2024).
128. Kecili, R. & Hussain, C. M. Chapter 4 - Mechanism of Adsorption on Nanomaterials. in (ed. Hussain, C. M. B. T.-N. in C.) 89–115 (Elsevier, 2018). doi:https://doi.org/10.1016/B978-0-12-812792-6.00004-2.
129. Pimentel, R. L. G. Adsorção de cromo vi utilizando carvão ativado produzido do mesocarpo do coco verde. (2018).
130. Sarabia, L. A. & Ortiz, M. C. 1.12 - Response Surface Methodology. in (eds. Brown, S. D., Tauler, R. & Walczak, B. B. T.-C. C.) 345–390 (Elsevier, Oxford, 2009).

doi:https://doi.org/10.1016/B978-044452701-1.00083-1.
131. Nair, A. T., Makwana, A. & Ahammed, M. The use of response surface methodology for modelling and analysis of water and wastewater treatment processes: A review. Water Sci Technol 69, 464–478 (2014).
132. Bennini, M. A. et al. Characterization and combustion of olive pomace in a fixed bed boiler: Effects of particle sizes. International Journal of Heat and Technology 37, 229–238 (2019).
133. Fernandes, M. C. et al. Bioethanol production from extracted olive pomace: dilute acid hydrolysis. Bioethanol 2, (2016).
134. Miranda, T. et al. Characterization and combustion of olive pomace and forest residue pellets. Fuel Processing Technology 103, 91–96 (2012).
135. Al-Widyan, M. I., Tashtoush, G. & Hamasha, A. M. Combustion and emissions of pulverized olive cake in tube furnace. Energy Convers Manag 47, 1588–1596 (2006).
136. Chouchene, A., Jeguirim, M., Khiari, B., Trouve, G. & Zagrouba, F. Study on the emission mechanism during devolatilization/char oxidation and direct oxidation of olive solid waste in a fixed bed reactor. J Anal Appl Pyrolysis 87, (2010).
137. Thommes, M. et al. Physisorption of gases, with special reference to the evaluation of surface area and pore size distribution (IUPAC Technical Report). Pure and Applied Chemistry 87, 1051–1069 (2015).
138. Braham, S., Taleb, Z., Djeziri, S. & Djellouli, H. Kinetic and isotherm evaluation of o-cresol adsorption on activated carbon procured from olive pomace. Acta Periodica Technologica (2023) doi:10.2298/APT2354137C.
139. Bennini, M. A. et al. Characterization and combustion of olive pomace in a fixed bed boiler: Effects of particle sizes. International Journal of Heat and Technology 37, 229–238 (2019).
140. Zaini, M. A. A., Zakaria, M., Mohd.-Setapar, S. H. & Che-Yunus, M. A. Sludge-adsorbents from palm oil mill effluent for methylene blue removal. J Environ Chem Eng 1, 1091–1098 (2013).
141. De Costa, P. D., Furmanski, L. M. & Dominguini, L. Production, characterization and application of activated carbon from nutshell for adsorption of methylene blue. Revista Virtual de Quimica 7, 1272–1285 (2015).
142. Bait, N., mokrani, T., Akkari, I., Ladji, R. & Bachari, K. Phenol adsorption onto olive pomace activated carbon: modelling and optimization. Naukovyi Visnyk Natsionalnoho Hirnychoho Universytetu (2023) doi:10.33271/nvngu/2023-2/125.
143. Abdel-Ghani, N. T., Rawash, E. S. A. & El-Chaghaby, G. A. Equilibrium and kinetic study for the adsorption of p-nitrophenol from wastewater using olive cake based activated carbon. Global Journal of Environmental Science and Management 2, 11–18 (2016).
144. Deng, S. et al. Enhanced adsorption of perfluorooctane sulfonate and perfluorooctanoate by bamboo-derived granular activated carbon. J Hazard Mater 282, 150–157 (2015).
145. Paiva, L., Silva, N., de Albuquerque, T., Silva, R. & Rocha, M. Estudo do aproveitamento do bagaço de caju residual da produção de xilitol como adsorvente do corante reativo azul bf-r. (2015). doi:10.5151/chemeng-cobeq2014-1138-20792-155114.

146. Heylmann, K. K. A. et al. Production, characterization, and application of activated charcoal from peach kernel in textile effluent treatment. Engenharia Sanitaria e Ambiental 26, 485–494 (2021).
147. Zeni, M., Thürmer, M. B., Poletto, P., Marcolin, M. & Ferreira, D. G. Autor para correspondência: Preparação e Caracterização de Membranas Assimétricas de Poli (Fluoreto de Vinilideno) Suportadas em Poliéster-I: Efeito do Tratamento Térmico nas Propriedades das Membranas. (2010) doi:doi.org/10.1590/S0104-14282010005000037.
148. Dorneles, K. R., Silva, W. R. & Reis, M. H. M. Purificação de compostos fenólicos do extrato de alfavaca (ocimum basilicum l.) Por filtração com membrana. (https://proceedings.science/p/159174?lang=pt-br.)